CELL BIOLOGY

A Direct and Functional Interaction Between G$_o$ and Rab5 During G Protein–Coupled Receptor Signaling

Vladimir Purvanov,[1] Alexey Koval,[1] Vladimir L. Katanaev[1,2]*

Rab5 is a small guanosine triphosphatase (GTPase) that regulates the early stages of endocytosis and is conserved in eukaryotes. Rab5 regulates the internalization of receptors and other membrane-associated signaling proteins. The function of Rab5 in these processes is considered relatively passive, so that the endocytic capacity of Rab5 is used during, for example, β-arrestin–dependent internalization of G protein (heterotrimeric guanine nucleotide–binding protein)–coupled receptors (GPCRs). Direct recruitment or activation of Rab5 by the components of these signaling pathways has not been reported. Here, we demonstrate an interaction of *Drosophila* Rab5 and an immediate transducer of GPCR signaling, the G protein G$_o$, in vitro and in vivo. Rab5 and G$_o$ bound to each other as purified proteins, as well as in fly extracts. In cellular assays, G$_o$ led to Rab5 activation and endosome fusion. We further showed that the G$_o$-Rab5 interaction functioned in *Drosophila* planar cell polarity and Wingless signal transduction, pathways initiated by GPCRs of the Frizzled (Fz) family. Additionally, the recycling Rab GTPases Rab4 and Rab11 functioned in Fz- and G$_o$-mediated signaling to favor planar cell polarity over canonical Wingless signaling. The interplay between heterotrimeric G proteins and Rab GTPases controlled receptor internalization, revealing a previously uncharacterized regulatory mechanism in GPCR signaling.

INTRODUCTION

Heterotrimeric guanine nucleotide–binding proteins (G proteins) are conserved in evolution from protozoa to mammals and function as molecular switches: They are active in the guanosine triphosphate (GTP)–bound state, which is terminated through their guanosine triphosphatase (GTPase) activity, thus adopting the inactive, guanosine diphosphate (GDP)–bound state. Heterotrimeric G proteins consist of the guanine nucleotide–binding α subunit and the βγ heterodimer. The GDP-bound trimeric complex can associate with G protein–coupled receptors (GPCRs), which, upon ligand binding, serve as guanine nucleotide exchange factors (GEFs) for Gα. This activity leads to the dissociation of Gα-GTP from βγ; both species can engage downstream effectors, thus transducing the signal from GPCRs (*1*). From insects to humans, Gα$_o$ is the predominant G protein α subunit in the nervous system (*2*, *3*). G$_o$ is required for proper brain function and development (*4*, *5*), as well as for the regulation of heart development and physiology (*6*, *7*). The crucial role of G$_o$ in transduction of the signals that emanate from the Frizzled (Fz) subfamily of GPCRs, which are important regulators of animal development, has been demonstrated in *Drosophila* and in vertebrate systems (*8–13*).

In contrast to heterotrimeric G proteins, small G proteins of the Ras family are monomeric. This family is composed of several subfamilies that control various aspects of cellular activities; the Rab subgroup regulates vesicular trafficking (*14*). Among the Rab family members, Rab5 controls early endocytic events, such as formation of clathrin-coated vesicles, fusion of endocytic vesicles and early endosomes, and homotypic fusion between early endosomes (*14*). Whereas Rab5 is crucial for the internalization of GPCRs, the opposing action is performed by the two recycling Rabs, Rab4 and Rab11 (*15*, *16*). Rab4 mediates fast recycling from early and sorting endosomes, whereas Rab11 regulates recycling endosomes, which ensure a slower kinetics of GPCR transport back to the plasma membrane (*14*, *17*). Although internalization of GPCRs typically serves to terminate their signaling, in several cases endocytosis is required for receptor signaling (*18*, *19*). In this regard, signaling by the Fz family of receptors is an interesting example.

Fz proteins initiate at least two branches of signaling pathways. The first is the so-called canonical pathway, which involves the co-receptor low-density lipoprotein receptor–related protein 5 or 6 and the axin-based protein complex that includes adenomatous polyposis coli, glycogen synthase kinase 3β, and casein kinase. This pathway culminates in the β-catenin–dependent transcription of target genes to specify cell fate in development (*20*). In *Drosophila*, this pathway is induced by the ligand Wingless (Wg) (*21*, *22*), a member of the Wnt family of secreted glycolipoproteins (*20*), and will be referred to herein as the Wg branch. The second type of signaling that emanates from Fz proteins uses a different set of transducer proteins and culminates in the regulation of cytoskeletal structures (*23*). This signaling pathway regulates convergent extension in vertebrates (*24*) and planar cell polarity (PCP) in flies (*25*), and will be referred to herein as the PCP branch of Fz signaling. In PCP, cells become uniformly polarized in the plane of the tissue, perpendicular to the better-known apico-basal polarization axis, responding to external polarity cues by reorganization of their cytoskeleton (*24*, *25*). In *Drosophila*, Fz1 and Fz2 are redundantly used in Wg signaling (*26*), whereas only Fz1 is involved in the PCP pathway (*27*). Both pathways rely on the G protein G$_o$ as the immediate transducer of Fz signals in *Drosophila* (*11*, *28*).

Both branches of Fz signaling depend on endocytosis. Regulated internalization of Fz1 is necessary to establish PCP (*29*). In *Drosophila*, Fz1 accumulates at the distal tips of wing cells to establish the sites of growth

[1]Department of Biology, University of Konstanz, Universitätsstrasse 10, Box 643, Konstanz 78457, Germany. [2]Institute of Protein Research, Russian Academy of Sciences, 4 Institutskaya Street, Pushchino 142290, Moscow Region, Russia.
*To whom correspondence should be addressed. E-mail: vladimir.katanaev@uni-konstanz.de

of actin-rich hairs (*30*). Fz1-containing endosomes move along microtubules that are aligned along the proximo-distal axis (*31*). Because both endocytosis and endosome motility on microtubules depend on Rab5 (*32*), this GTPase may play important roles in the establishment of PCP. Similarly, clathrin- and Rab5-dependent endocytosis is essential for activation of the Wg pathway in vitro (*33, 34*). A role for Rab5 was also investigated in the imaginal wing discs of *Drosophila* larvae (*34*). In this tissue, Wg signaling can be studied by monitoring the high-threshold Wg target gene *Senseless*, which is expressed close to the source of Wg production, and the low-threshold target gene *Distal-less*, which is expressed throughout the wing disc (*35*). Enhanced Wg signaling is required for the formation of the sensory bristles that decorate the adult wing margin; ectopic bristles are produced by strong overactivation of the pathway (*36–38*). Rab5 is necessary for the expression of *Senseless* and the formation of sensory bristles, whereas the expression of *Distal-less* is less dependent on Rab5 (*34*). On the basis of these observations, it was concluded that low-intensity Wg signaling could be induced from the plasma membrane, whereas high-intensity Wg signaling could emanate from endosomes that contained complexes of Wg and Fz (*34*). In addition to internalizing the ligand-receptor complexes, endocytosis may additionally be involved in more downstream steps of the Wg-Fz signaling (*33*). Here, we demonstrate a physical and functional interaction between G_o and Rab GTPases. We further show the importance of this interaction for the Wg and PCP branches of Fz signaling in *Drosophila*. Our results unravel a general G_o- and Rab-dependent mechanism of regulation in GPCR-mediated signal transduction.

RESULTS

Rab5 is involved in the Wg and PCP branches of Fz signaling

Rab5 null loss-of-function cells lose apico-basal polarity and form neoplastic tumors in *Drosophila* (*39*), preventing the analysis of the role of Rab5 in Fz signaling in epithelia. To partially inhibit Rab5 function, we expressed the dominant-negative Rab5 construct Rab5[S43N] or an RNA interference (RNAi)–targeting construct in *Drosophila* wings. In accordance with previous observations (*34*), we found that the wing margins, which normally are decorated by sensory bristles (Fig. 1A), were frequently lost in wings expressing Rab5[S43N] (Fig. 1B), which is a characteristic sign of reduced Wg signaling (*36*). A similar phenotype was produced by the Rab5-specific RNAi (Fig. 1C). We also analyzed the expression of Wg target genes in wing imaginal discs of wild-type larvae (fig. S1, A to C) and larvae expressing Rab5[S43N] (fig. S1, D to F) or Rab5-RNAi (fig. S1, G to I). We found that expression of the short-range target *Senseless* was frequently undetectable in cells of the Rab5[S43N]- or Rab5-RNAi–expressing discs (fig. S1, E and H), whereas expression of the long-range target *Distal-less* was unaffected (fig. S1, D and G). Thus, Rab5 appeared to be necessary for high-intensity Wg signaling. On the other hand, the increased abundance of Rab5 in wings, especially of its constitutively active form Rab5[Q88L], resulted in the increased activation of the Wg pathway relative to that in wings from wild-type flies, as determined by the appearance of multiple ectopic margin bristles away from the normal zone of production (Fig. 1, D to F).

We also found that inhibition of Rab5 led to defects in the establishment of PCP (Fig. 1, G and H). These PCP defects were not a secondary effect of loss of the wing margin, because direct inhibition of Wg signaling resulted in loss of wing margins but not in PCP phenotypes (Fig. 1I). An increase in the abundance of Rab5 also led to defects in PCP, which were relatively mild and involved the induction of multiple wing hairs (Fig. 1J); this phenotype can be induced by mislocalization of Fz1 (*40*). Thus, Rab5 is involved in both the Wg and the PCP branches of Fz signaling in *Drosophila*.

Rab5[Q88L] was more potent than wild-type Rab5 in inducing the formation of ectopic bristles (Fig. 1, E and F).

Fz proteins stimulate endocytosis in cis

The involvement of Rab5 in Fz signaling suggests that Fz may have a general function in the regulation of endocytosis. To investigate this possibility, we expressed Fz2 in *Drosophila* hemocytes and performed pulse-chase endocytosis experiments with Texas Red–labeled dextran (a fluorescent marker for endocytosis) in these cells and in control cells. Whereas control hemocytes internalized only small amounts of dextran during the 20-min chase (Fig. 2, A and B), cells that had Fz2 exhibited an enhanced uptake of dextran, as determined both by the numbers of dextran-containing intracellular vesicles and by the intensity of fluorescence within them (Fig. 2, C to F).
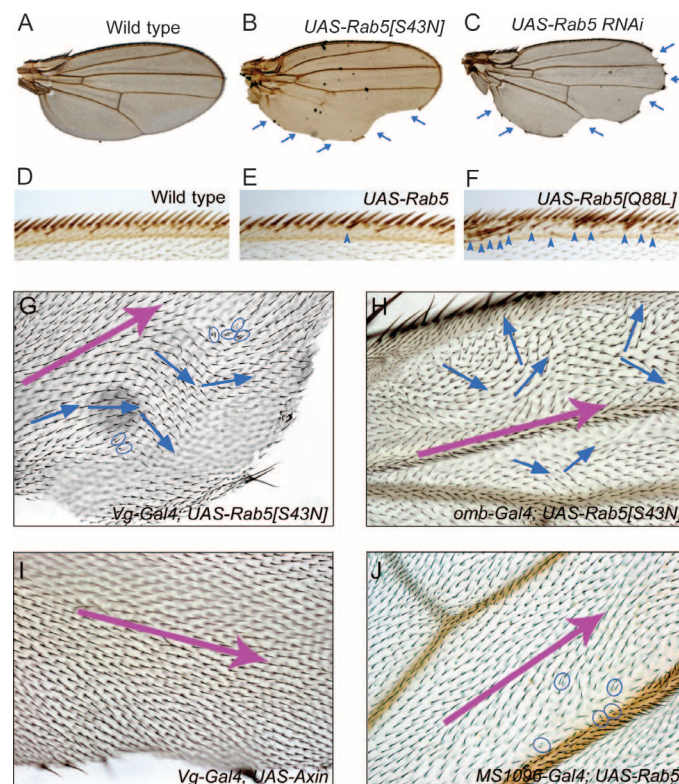

Fig. 1. Inhibition and enhanced activation of Rab5 produce Wg and PCP phenotypes. (**A**) Wing from a wild-type fly. (**B** and **C**) Inhibition of Rab5 by expressing the dominant-negative construct (B) or RNAi targeting Rab5 (C) with *Vg-Gal4* results in loss of the wing margin structures (arrows). (**D**) Magnification of a region of wing margin shown in (A). (**E** and **F**) Overexpression of wild-type (E) or constitutively active Rab5 (F) with *MS1096-Gal4* results in the appearance of ectopic margin bristles (arrowheads). (**G** and **I**) Expression of dominant-negative Rab5 (G) by the *Vg-Gal4* driver results in loss of wing margin structures and PCP defects. These include deviations of hair orientation (blue arrows) from the main proximo-distal direction (big magenta arrow) and the appearance of multiple wing hairs (blue ovals). Similar expression of the Wg pathway inhibitor (AxinΔRGS) results in loss of the wing margin but not in PCP defects (I). (**H**) Expression of another Rab5 dominant-negative construct, Rab5[S43N]-YFP, by another driver (*omb-Gal4*) also results in PCP defects. (**J**) Overexpression of Rab5 also results in mild PCP defects (blue ovals).

This stimulation of endocytosis reflected the basal activity of *Drosophila* Fz2, because the addition of purified Wg resulted in only a small (although significant) additional increase in the uptake of dextran (Fig. 2C). Fz1 also revealed a capacity to stimulate endocytosis (fig. S2, A to G). The basal (ligand-independent) activity of Fz1 was much more modest than that of Fz2; instead, Fz1 was much more responsive to stimulation by Wg (fig. S2, C to G).

We next asked whether Fz proteins increased the overall endocytic capacity of the cell. An alternative possibility was that Fz proteins strongly stimulated their own internalization and that dextran was taken up with Fz. We reasoned that if the first option were true, a substantial fraction of dextran-containing intracellular structures should be devoid of Fz. However, we found that most of the dextran-positive structures contained Fz2 tagged with green fluorescent protein (Fz2-GFP) (Fig. 2, D to F). From a total of

Fig. 2. Fz induces endocytosis and Rab5 activation in hemocytes and interacts with Rab5 in vitro. (**A** to **F**) Endocytosis was studied by monitoring the uptake of Texas Red–conjugated dextran in control (A and B) or Fz2-GFP–expressing (D to F) hemocytes. In Fz2-expressing cells, most dextran-positive vesicles contained Fz2-GFP (white arrows; arrowheads mark vesicles that lack Fz2). (C) Quantification of dextran-containing structures in different genotypes. Data are shown as the mean ± SEM. Sample size was 60 to 100 hemocytes. Statistical significance is shown with *P* values (determined by Student's *t* test). (**G** and **H**) Rab5-GFP expressed in hemocytes with *Cg-Gal4* exhibited diffuse localization (G), whereas activated Rab5[Q88L]-YFP induced the formation of giant endosomes that appeared as doughnut-type structures (H, arrows). (I) Coexpression of Fz2 forces Rab5-GFP to form giant endosomes (arrows). The fluorescence of Fz2-GFP was less intense than that of Rab5-GFP and its input was negligible to the combined signal. The green channel intensity settings in (G) to (I) are reduced compared to those in (E). (J) Quantification of giant, Rab5-containing endosomes per hemocyte in the different genotypes presented as in (C). Sample size was 10 to 39 hemocytes. (**K**) Matrix-immobilized Rab5 was used to pull down MBP-tagged Fz1 or Fz2. An unrelated GPCR, 5HT2c, did not interact with Rab5. (**L**) Fz proteins, with or without Wg, failed to stimulate GTP binding by Rab5. CG9139 (*Drosophila* Rabex5) activated Rab5 when provided at only 2% of the amount of Rab5. The data are presented as the percentage of maximal fluorescence for better comparison.
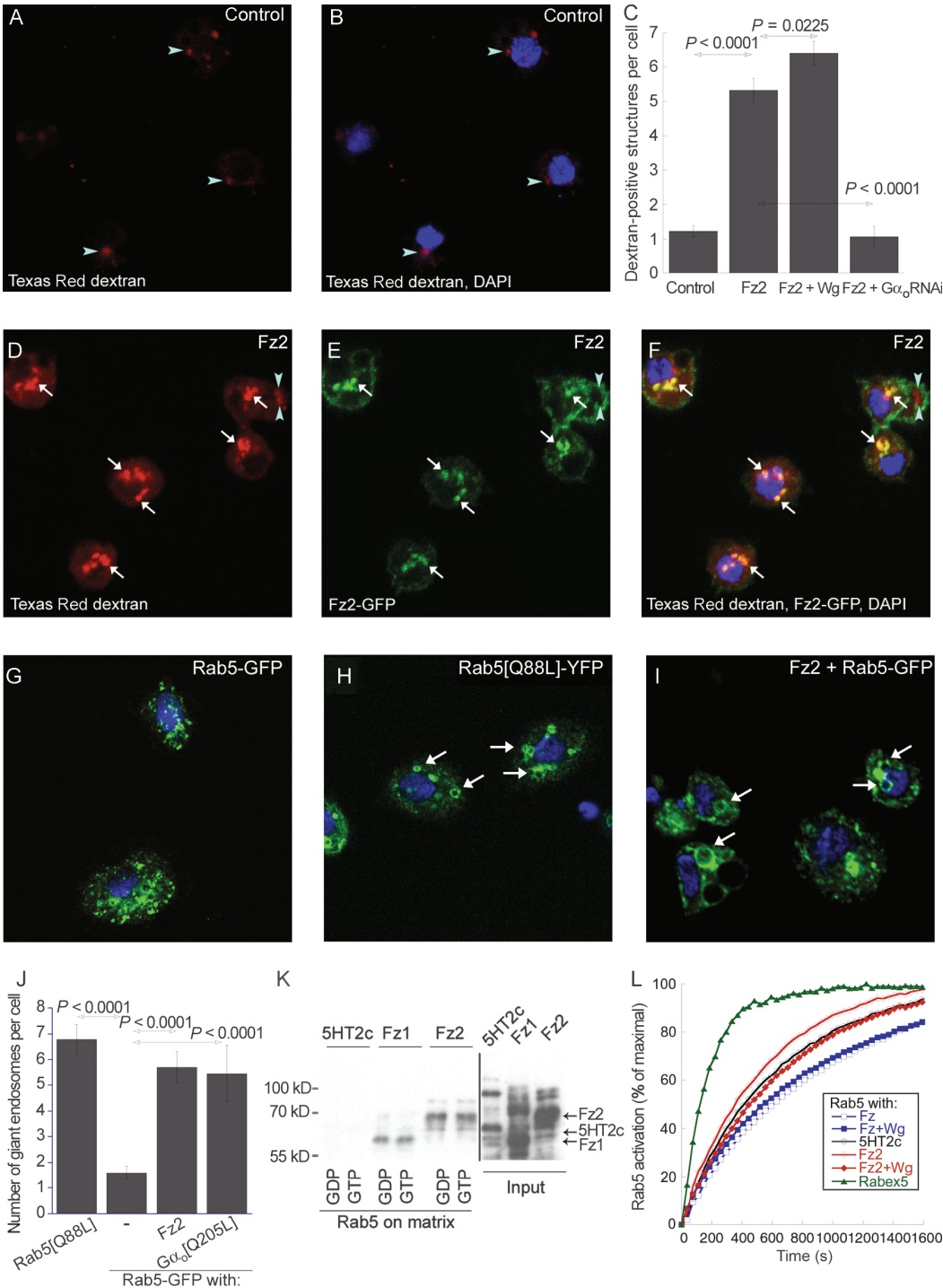
311 dextran-containing vesicles analyzed in several hemocyte preparations, 228 (73%) also contained Fz2-GFP. This correlated well with the overall stimulation of dextran uptake by Fz2; endocytosis in the control hemocytes was 15% of that in the cells that contained Fz2 (Fig. 2C). Thus, it appears that most of the additional dextran-containing vesicles that were induced by Fz2 also contained Fz2. In other words, the presence of Fz2 stimulated endocytosis in cis, which stimulated the internalization of Fz2. These data also suggested that Fz2 activated endocytosis either directly or through intermediates acting in the vicinity of the receptor.

Fz proteins activate Rab5 in vivo but not in vitro

Because Fz2 stimulated endocytosis in cis and Rab5 was necessary for Fz signaling, we hypothesized that Fz proteins could activate Rab5. We expressed GFP or yellow fluorescent protein (YFP) fusions of wild-type Rab5 or the constitutively active mutant Rab5, Rab5[Q88L], in *Drosophila* hemocytes and compared their localization patterns. Wild-type Rab5-GFP exhibited a diffuse, weakly punctate pattern (Fig. 2G). In contrast, expression of Rab5[Q88L]-YFP led to extensive fusion of endosomes that resulted in the formation of giant endosomes, which appeared as doughnut structures (Fig. 2H), as reported previously in other cellular assays (*41*). The coexpression of Fz2 with wild-type Rab5-GFP led to the formation of Rab5-containing giant endosomes (Fig. 2, I and J), which demonstrated that Fz2 could activate Rab5 in this cellular assay.

Rab5 interacts directly with angiotensin II type 1A receptor, a GPCR (*42*). Therefore, we investigated whether Rab5 could physically interact with Fz proteins. We expressed Fz1 and Fz2 as maltose-binding protein (MBP) fusion proteins in bacterial membranes to produce biologically active receptors (*43*), in parallel with an unrelated GPCR (human 5HT2c). We also prepared Rab5 as a hexahistidine (His_6)–tagged protein and covalently attached it to CNBr-Sepharose. His_6-tagged Rab5, either in its GDP-loaded or in its guanosine 5′-O-(3′-thiotriphosphate) (GTP-γ-S)–loaded conformation, bound to Fz1 and Fz2, but not to the control receptor (Fig. 2K), which demonstrates a physical interaction between Fz proteins and Rab5. The activation of G proteins by GPCRs can be studied in vitro (*43*, *44*). To test whether Fz proteins might directly activate Rab5, we designed an in vitro assay in which the incorporation of a GTP analog into recombinant Rab5 was tested by fluorescence measurements (*45*). The addition of detergent-solubilized Fz1 or Fz2, in the presence or absence of Wg, failed to increase the speed of GTP binding by Rab5 compared to that under control conditions (Fig. 2L). In contrast, the addition of recombinant CG9139, a *Drosophila* homolog of the Rab5 GEF Rabex5 (*46*), efficiently stimulated the incorporation of GTP into Rab5 (Fig. 2L). We thus conclude that Fz proteins do not directly activate Rab5 but must have an intermediate activator; the physical binding between Fzs and Rab5 might reflect the capacity of Rab5 to induce the internalization of Fz in vivo.

Activation of endocytosis by Fz proteins is $G\alpha_o$-dependent

Because G_o is a direct binding partner and transducer of Fz proteins in *Drosophila* and mammalian cells (*8–13*), we hypothesized that G_o might serve as a link between Fz and Rab5. The α subunit of G_o ($G\alpha_o$) plays a functional role in insect hemocytes (*47*). We found that RNAi-mediated knockdown of $G\alpha_o$ reduced the uptake of dextran by Fz1-expressing (fig. S2, G to K) and Fz2-expressing hemocytes (Figs. 2C and 3, A and B). The few dextran-positive vesicles that remained in the Fz2-expressing cells did not colocalize with Fz2-GFP (Fig. 3B), confirming that $G\alpha_o$-specific RNAi reduced the extent of endocytosis of Fz2 to that observed in the control hemocytes lacking Fz2 (Fig. 2C). Large amounts of Fz2-GFP were still internalized into these cells. Multiple routes for the internalization of Fz exist (*48*); our data indicate that $G\alpha_o$ controls only one of these routes—a route

that leads to a noticeable stimulation of endocytosis as judged by the marked uptake of dextran.

$G\alpha_o$ binds to Rab GTPases

A yeast two-hybrid screen of the *Drosophila* genome found a low-confidence interaction between Rab5 and $G\alpha_o$ (*49*). To confirm this interaction, we purified these proteins after they were expressed in bacteria. We also produced recombinant Rab4 and Rab11 proteins. In pull-down experiments with glutathione *S*-transferase (GST)–tagged Rab proteins and His_6-tagged $G\alpha_o$, Rab5 and Rab4 displayed robust binding to $G\alpha_o$ (Fig. 3, C and D), whereas the binding of Rab11 to $G\alpha_o$ was less pronounced (and was not investigated further). Whereas Rab4 revealed no nucleotide preference in its interaction with $G\alpha_o$, Rab5-GDP was reproducibly a better binding partner for $G\alpha_o$ than was Rab5-GTP (Fig. 3D).

To investigate the Rab5-$G\alpha_o$ interaction in a different experimental system, we prepared Rab5 as a His_6-tagged protein and covalently attached $G\alpha_o$ to CNBr-Sepharose. In this system, Rab5 demonstrated robust binding to $G\alpha_o$ but not to control matrices (Fig. 3E). Similar interactions were observed when Rab5 was immobilized on a matrix and $G\alpha_o$ was applied in soluble form (Fig. 3F). Analysis of the nucleotide dependence of the Rab5-$G\alpha_o$ interaction revealed that GDP- and GTP-loaded forms of $G\alpha_o$ bound to Rab5 to a similar extent, whereas, as before, Rab5-GDP preferentially bound to $G\alpha_o$ under certain binding conditions (Fig. 3, E and F).

To determine whether endogenous Rab5 and $G\alpha_o$ proteins could interact, we showed that Rab5 produced in *Drosophila* was efficiently precipitated by $G\alpha_o$-containing matrices but not by control matrices (Fig. 3G). Similarly, endogenous or overexpressed $G\alpha_o$ from *Drosophila* was an effective binding partner for Sepharose-immobilized Rab5. As before, $G\alpha_o$ bound more strongly to Rab5-GDP than to Rab5-GTP (Fig. 3H). Thus, recombinant and endogenous forms of Rab5 and $G\alpha_o$ bound to each other. $G\alpha_o$ also interacted with the fast-recycling Rab4 protein but not with the slow-recycling Rab11 protein. Because $G\alpha_o$ interacts with Fz proteins in biochemical assays (*43*), we investigated whether the presence of $G\alpha_o$ could affect interactions between Fz and Rab5. We found that $G\alpha_o$ did not substantially affect the ability of Fz1 to bind to Rab5 (fig. S3A), which suggested that the binding of Fz to these two G proteins might occur through different sites on the receptor, potentially enabling the formation of a tertiary complex among Fz, $G\alpha_o$, and Rab5.

To determine whether $G\alpha_o$ can directly activate Rab5, we performed in vitro Rab5 activation experiments. The addition of excessive concentrations of GTP-γ-S–loaded $G\alpha_o$ resulted in only a slight increase in the amount of GTP that was bound to Rab5 relative to that in the control conditions, whereas Rabex5 (CG9139) markedly accelerated the rate of incorporation of GTP (Fig. 3I). The direct binding of $G\alpha_o$ to Rab GTPases (Fig. 3, C to H) represents the second example of a direct interaction between heterotrimeric and small G proteins. The previously described case is the interaction of the Ras family small G protein AGS1 (activator of G protein signaling 1) with $G\alpha_i$ and $G\alpha_o$ proteins (*50*). AGS1 activates heterotrimeric G proteins in vivo (*51*) and in vitro by directly stimulating the incorporation of GTP into the α subunit (*50*). In contrast, Rab5 failed to stimulate GTP loading by $G\alpha_o$ (fig. S3B). Thus, we conclude that $G\alpha_o$ and Rab5 do not directly activate each other.

## GTP-loaded $G\alpha_o$ activates Rab5 in vivo

We found that in some conditions, $G\alpha_o$ preferably bound to Rab5-GDP rather than to Rab5-GTP (Fig. 3, D, E, and H). This preference may hint at the potential activating capacity of $G\alpha_o$ to Rab5. To investigate whether $G\alpha_o$ could affect the activity of Rab5, we coexpressed the activated mutant form of $G\alpha_o$, $G\alpha_o$[Q205L], with wild-type Rab5-GFP in hemocytes and found Rab5-containing giant endosomes (Figs. 2J and 3J), similar to those

induced by the expression of Rab5[Q88L]-YFP (Fig. 2H) or by the co-expression of Fz2 with Rab5-GFP (Fig. 2, I and J), which demonstrated that $G\alpha_o$ could activate Rab5 in this cellular assay. $G\alpha_o$[Q205L] colocalized with Rab5 in the giant endosomes (Fig. 3, J to L). We also observed that, even in the absence of overexpression of Rab5, endogenous Rab5 could be forced to form giant endosomes in $G\alpha_o$[Q205L]-expressing cells (fig. S4A) but not in control cells (fig. S4B). We also observed the formation of Rab5-containing giant endosomes by $G\alpha_o$[Q205L] and the colocalization of $G\alpha_o$ and Rab5 at these structures in experiments with another tagged form of Rab5, V5-Rab5 (fig. S4, C to E). Incubation with an antibody against $G\alpha_o$ also revealed the giant endosome–like structures in cells that contained $G\alpha_o$[Q205L] and endogenous Rab5 (fig. S4, F and G). Cumulatively, these

data demonstrate that the activated form of $G\alpha_o$ activated endogenous and exogenous Rab5 to stimulate the fusion of endosomes and the formation of giant endosomes, structures to which $G\alpha_o$ localized. Such endosomal localization of $G\alpha_o$ is similar to the previously reported localization of the activated α subunit of the yeast heterotrimeric G protein Gpa1 (52).

We also studied how $G\alpha_o$ affected Rab5 in *Drosophila* salivary glands. In these giant polyploid cells, wild-type Rab5-GFP showed a diffuse and weakly punctate pattern of localization, although it was also found at the plasma membrane (Fig. 4A). In contrast, Rab5[Q88L]-YFP was not found at the plasma membrane, but instead localized to large intracellular structures, possibly analogs of giant endosomes in this tissue (Fig. 4B). Similar to the situation that we observed in hemocytes, coexpression of $G\alpha_o$[Q205L]

Fig. 3. $G\alpha_o$ is required for Fz2-induced endocytosis and also binds to and activates Rab5. (A and B) Fz2-induced endocytosis was prevented by knockdown of $G\alpha_o$. The experiment was performed as described for Fig. 2, A to F. (C to H) Pull-down experiments with $G\alpha_o$ and Rab proteins were performed in solution with subsequent application to Ni-agarose (C and D) or with matrix-immobilized $G\alpha_o$ (E and G) or Rab5 (F and H). Purified proteins or extracts from wild-type *Drosophila* (H) or flies overexpressing V5-Rab5 (G) or $G\alpha_o$ (H) were applied to matrices. In all conditions, $G\alpha_o$ and Rab5 specifically bound to each other but not to control matrices, as detected with antibodies against His$_6$, V5, GST, or $G\alpha_o$. Proteins were preloaded with nucleotides as indicated; otherwise, they were loaded with GDP. Equal input of proteins was ensured by Coomassie staining of the input proteins; see (C) for an example. Each panel is a representative image of at least three independent experiments. (I) $G\alpha_o$ failed to stimulate GTP binding by Rab5. CG9139 (*Drosophila* Rabex5) provided at an equivalent amount strongly activated Rab5. (J to L) Hemocytes coexpressing activated $G\alpha_o$[Q205L] and Rab5-GFP forced Rab5-GFP to form giant endosomes (arrows), in which $G\alpha_o$ and Rab5 colocalized (arrows).
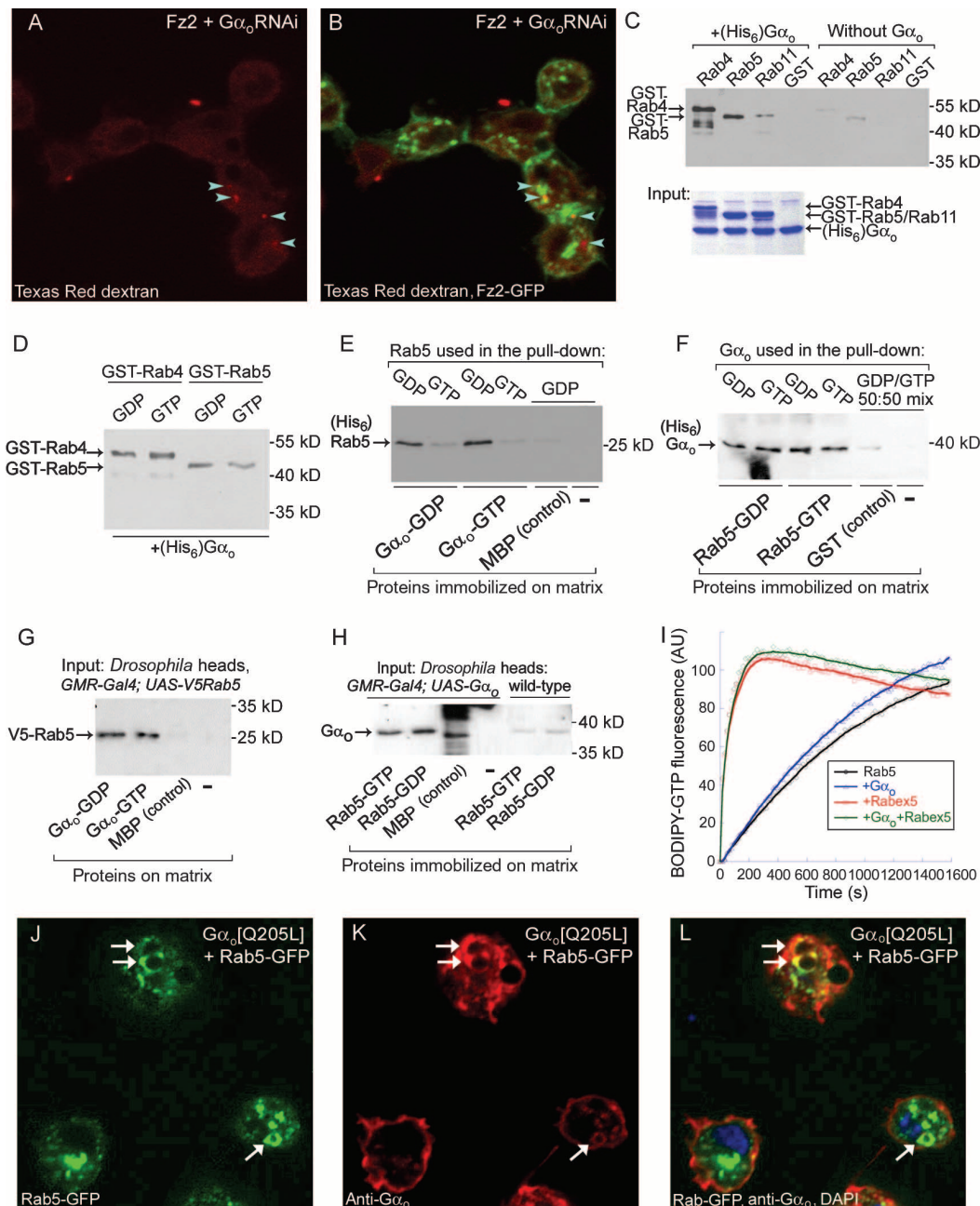
and wild-type Rab5-GFP forced the latter to adopt the activated pattern with a marked localization to large intracellular structures (Fig. 4C). Fz1 and Fz2 also induced a shift in the localization pattern of Rab5 to bring it into bright intracellular puncta that were reminiscent of those induced by Rab5[Q88L]-YFP in the salivary glands (fig. S5, A and B).

In contrast to expression of the activated form of $G\alpha_o$, expression of wild-type $G\alpha_o$ did not lead to the activation of Rab5. Wild-type $G\alpha_o$ failed to induce the formation of giant Rab5-containing endosomes in hemocytes (fig. S4, H to J); fluorescence microscopic analysis with antibody against $G\alpha_o$ showed no giant endosome–like pattern upon overexpression of wild-type $G\alpha_o$ in the presence (fig. S4H) or absence (fig. S4, K and L) of Rab5 overexpression. In salivary glands, wild-type $G\alpha_o$ did not substantially change the localization pattern of Rab5-GFP (Fig. 4D). Thus, only the activated, GTP-loaded form of $G\alpha_o$ led to the activation of Rab5 in vivo. How is this finding reconciled with the observation that both $G\alpha_o$-GDP and $G\alpha_o$-GTP efficiently bind to Rab5 in vitro? We propose that in vivo, $G\alpha_o$-GDP forms complexes with $G\beta\gamma$ by outcompeting other $G\alpha$ subunits (53) and is thus poorly available in a free form to interact with the target proteins. Indeed, purified $G\beta\gamma$ prevented Rab5 from binding to $G\alpha_o$-GDP in pull-down experiments (fig. S3C). Similar results were obtained with another $G\alpha_o$ target protein, axin, which interacts with both nucleotide-bound forms of $G\alpha_o$ in vitro, but only with the GTP-bound form of $G\alpha_o$ in salivary glands (54).

$G\alpha_o$ likely activates Rab5 by recruiting it to the plasma membrane

Because $G\alpha_o$ failed to activate Rab5 directly, we hypothesized that $G\alpha_o$ induced the activation of Rab5 through its recruitment to the plasma membrane, where Rab5 is activated by membrane-localized exchange factors (55). Indeed, $G\alpha_o$ and Rab5 colocalize in giant endosomes in hemocytes (Fig. 3, J to L, and fig. S4, C to E). But was this colocalization the cause or the consequence of Rab5 activation? To address this question, we used a non-activatable mutant form of Rab5, Rab5[S43N], that was tagged with YFP and analyzed whether its localization pattern changed upon coexpression with $G\alpha_o$[Q205L]. We detected Rab5[S43N]-YFP in the nucleus and the cytoplasm in salivary glands and hemocytes (Fig. 4E and fig. S4P). We do not know the reason for the nuclear localization of this form of Rab5, but a similar localization of this construct was reported in S2 cells (56). Co-expression of $G\alpha_o$[Q205L] (but not wild-type $G\alpha_o$) resulted in a substantial relocalization of Rab5[S43N]-YFP to the plasma membrane in salivary glands (Fig. 4, E to H), where $G\alpha_o$ was localized (54). To quantify the extent of this relocalization, we analyzed the presence and absence of Rab5[S43N]-YFP from cell-to-cell borders of salivary glands. In the control glands, only ~25% of such borders showed a clear localization of Rab5[S43N]-YFP, whereas ~50% of all borders were completely devoid of Rab5[S43N]-YFP (Fig. 4, E and H). Coexpression of $G\alpha_o$[Q205L], but not wild-type $G\alpha_o$, reverted this ratio (Fig. 4, E to H).
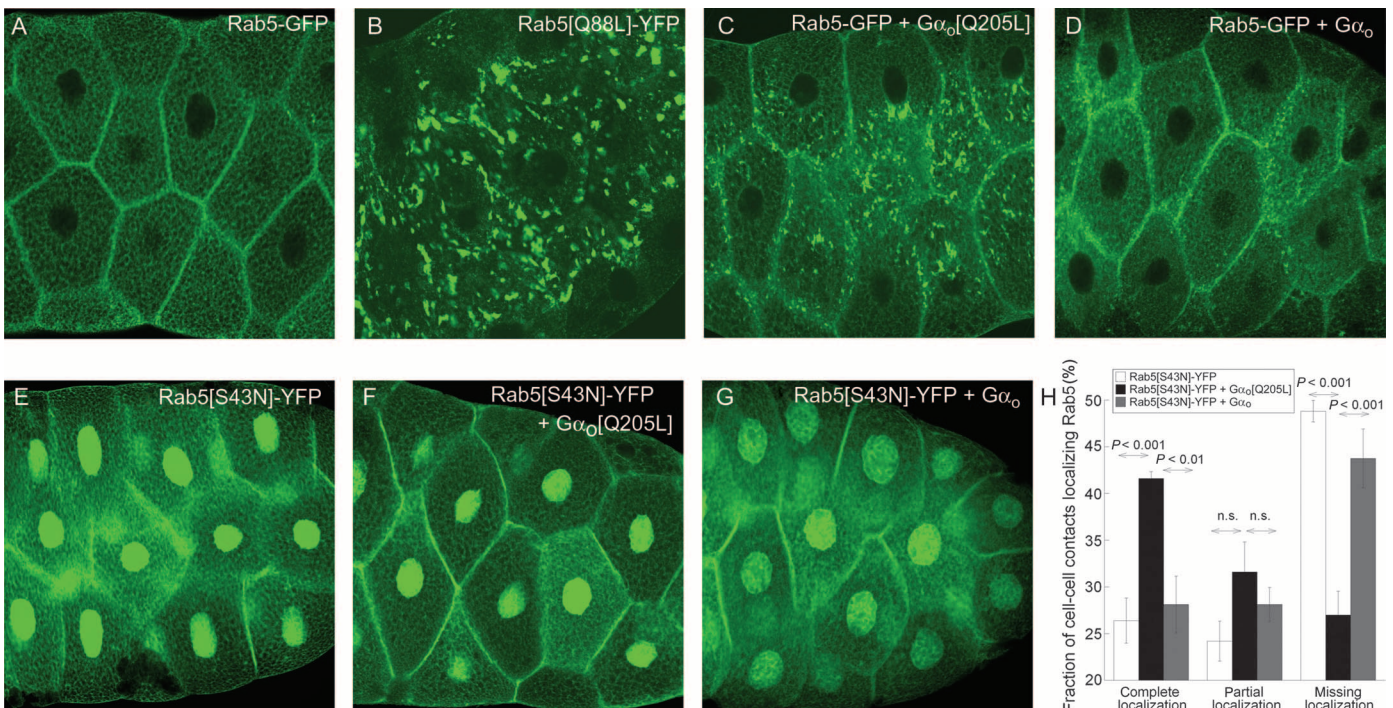
Fig. 4. $G\alpha_o$ activates Rab5 in salivary glands. (**A** and **B**) Rab5-GFP expressed in *Drosophila* salivary glands with *71B-Gal4* was localized to the plasma membrane and diffusely through the cytoplasm (A), unlike constitutively activated Rab5[Q88L]-YFP, which localized to giant cytoplasmic structures (B). (**C** and **D**) Coexpression of $G\alpha_o$[Q205L] (C) but not wild-type $G\alpha_o$ (D) forced Rab5-GFP to adopt the activated pattern of localization in giant cytoplasmic structures, with some remaining plasma membrane localization. (**E to H**) Rab5[S43N]-YFP (the nonactivatable form of Rab5) was most abundant in the nucleus and cytoplasm and least abundant at the plasma membrane (E). $G\alpha_o$[Q205L] induced the partial relocalization of Rab5[S43N]-YFP to the plasma membrane (F), whereas wild-type $G\alpha_o$ did not (G). (H) Quantification of Rab5[S43N]-YFP at the cell-to-cell contacts. The percentage of cell-to-cell contacts that exhibited complete localization of Rab5[S43N]-YFP increased from ~25 to ~40%, whereas the percentage of cell-to-cell contacts that were completely devoid of Rab5[S43N]-YFP decreased from ~50 to ~25% in the presence of $G\alpha_o$[Q205L]. Sample size was five glands (~30 cells per gland) for each genotype. Data are shown as for Fig. 2C. Two-way analysis of variance (ANOVA) was used to determine significance. n.s., not significant.

Activated $G\alpha_o$ exhibited intense localization in punctate (possibly vesicular) and giant endosome–like structures in hemocytes (fig. S4, F and G). When $G\alpha_o$[Q205L] was coexpressed with Rab5[S43N]-YFP, the localization pattern of the latter changed (fig. S4, M to Q). Specifically, Rab5[S43N]-YFP was observed in discrete puncta instead of exhibiting a diffuse cytoplasmic localization. These puncta also contained $G\alpha_o$ (fig. S4, M to O). Certain giant endosome–like structures were still observed by fluorescence microscopic analysis with an antibody against $G\alpha_o$ in these hemocytes (fig.

S4M), similar to that observed in hemocytes expressing $G\alpha_o$[Q205L] alone (fig. S4F). We could not quantitatively determine whether the number of such structures decreased upon coexpression of Rab5[S43N]-YFP; however, we noticed that when these structures were visible, they were devoid of Rab5[S43N]-YFP (fig. S4, M to O). In S2 cells, Rab5[S43N]-YFP was largely desegregated from endosomes that contained wild-type Rab5 (56). Thus, it seems plausible that $G\alpha_o$[Q205L] was capable of interacting with endogenous Rab5 or overexpressed Rab5[S43N]-YFP in hemocytes. In the case of the former interaction, the activation of Rab5 was followed by the fusion of endosomes into giant endosomes, whereas in the latter case, $G\alpha_o$[Q205L] induced the relocalization of Rab5[S43N]-YFP into $G\alpha_o$-containing puncta (fig. S4N). Wild-type $G\alpha_o$ was unable to change the localization of Rab5[S43N]-YFP in hemocytes (fig. S4, R to T). The combined analysis of the relocalization of Rab5[S43N]-YFP in salivary glands and hemocytes led us to conclude that GTP-loaded $G\alpha_o$ bound to Rab5 and mediated its translocation from the cytoplasm to membrane compartments. We predict that this recruitment is the first step in the activation of Rab5, the second step being the GTP loading of Rab5 with the help of membrane-localized Rab5 GEF proteins (55).

Recycling Rabs are differentially involved in the Wg and PCP branches of Fz signaling

Our data so far suggested that Fz- and $G\alpha_o$-mediated activation of Rab5 resulted in the local induction of endocytosis and the internalization of Fz proteins. Because Rab5 participates in the Wg and PCP branches of Fz signaling during wing development in *Drosophila* (Fig. 1), we next analyzed the physiological importance of the internalization of Fz in this tissue. Rab5-dependent internalization of the Wg-Fz complexes to endosomes is thought to be required for the full extent of the Wg-Fz signaling (34). We thus predicted that the forced recycling of these complexes back to the plasma membrane would reduce the extent of their signaling. Indeed, we found that the expression of the activated forms of Rab4 (Rab4[Q67L]) or Rab11 (Rab11[Q70L]) suppressed
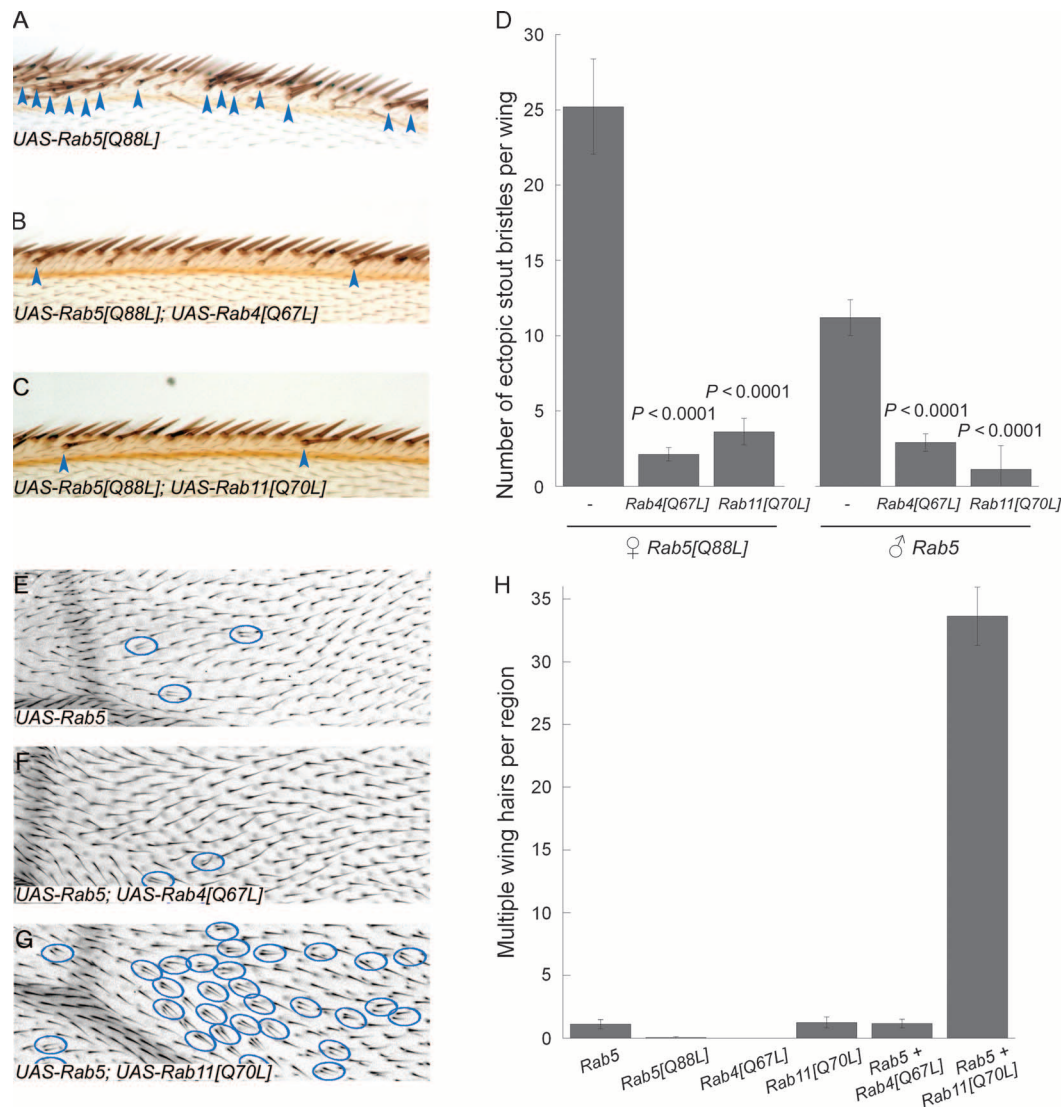

Fig. 5. Recycling Rab proteins show different effects on Rab5-mediated activation of the Wg and PCP pathways. (A to D) Ectopic margin bristles (arrowheads) induced by activated Rab5 (A) were strongly suppressed by coexpression of the activated forms of Rab4 (B) or Rab11 (C). (D) Quantification of the ectopic bristles induced by Rab5[Q88L] or wild-type Rab5 in different genotypes. Ectopic bristles were analyzed in male flies expressing wild-type Rab5 because the phenotypes in female flies were less prevalent as a result of the use of the X-linked driver (*MS1096-Gal4*). Sample size was 14 to 19 wings. Data are shown as for Fig. 2C. (E to H) Multiple wing hairs (blue ovals) induced by the *MS1096-Gal4*–driven expression of Rab5 (E) were unaffected by coexpression of activated Rab4 (F) but were increased in number upon coexpression of activated Rab11 (G). (H) Quantification of multiple wing hairs induced by the expression and coexpression of different forms of Rab5, Rab4, and Rab11. Sample size was 12 to 19 wings. Data are shown as for Fig. 2C.

the ability of Rab5 to enhance activation of the Wg pathway (Fig. 5, A to D), whereas the recycling Rabs alone did not produce any phenotype.

In contrast, we observed a very different effect of the recycling Rabs on the ability of Rab5 to influence PCP-Fz signaling. Whereas coexpression of Rab4[Q67L] with Rab5 had almost no effect on PCP, coexpression of Rab11[Q70L] and Rab5 produced a marked multiple wing hair phenotype (Fig. 5, E to H). Such multiple wing hairs can be produced by late overexpression of Fz1, which induces the formation of ectopic hair initiation sites. This phenotype can be used as a readout of the increased stimulation of Fz1 signaling to the actin cytoskeleton in PCP (40, 57). Thus, recycling of endosomes seemed to suppress the enhanced activation of the Wg pathway but to promote the PCP branch of signaling.

Rab proteins and Gα$_o$ cooperate in the PCP branch of Fz signaling

The multiple wing hair phenotype can also be induced by overexpression of Gα$_o$ or its activated form (11). To test whether Gα$_o$ genetically interacted in PCP signaling with Rab GTPases, we performed coexpression experiments in *Drosophila* wings. We found that coexpression of Rab5 strongly enhanced the number of multiple wing hairs induced by Gα$_o$ (Fig. 6, A and B). Among the activated Rabs, Rab4 and Rab5 both induced a factor of 2 to 3 increase in the number of multiple wing hairs, whereas activated Rab11 induced a factor of 20 enhancement in the number of multiple wing hairs (Fig. 6, C and D). The activated form of Gα$_o$ was also stimulated in the presence of overexpressed Rab5 (Fig. 6E). Moreover, we found that the potency of Gα$_o$ to induce the formation of multiple wing hairs was decreased upon removal of one gene copy of *Rab5* (Fig. 6E). These observations indicate that Rab5 may be one of the targets of Gα$_o$ in the PCP-Fz pathway. Furthermore, the synergism between Gα$_o$ and Rab11 implicates Rab5-mediated endocytosis and Rab11-mediated recycling in PCP-Fz signaling.

Rab5 and Gα$_o$ negatively cooperate in the Wg branch of Fz signaling

We showed that Gα$_o$ bound to Rab5 and Rab4, thus possibly promoting the endocytosis and fast recycling of GPCRs. On the other hand, the recycling Rabs impaired the enhanced activation of the Wg branch of Fz signaling. We wondered what the interplay between Rab5 and Gα$_o$ could be in this pathway. Whereas Gα$_o$ is required for Wg signaling in *Drosophila*, excessive activation of Gα$_o$ enhances the expression of the low-threshold Wg target gene *Distal-less*, but not the high-threshold target gene *Senseless* (11). Thus, we hypothesized that Gα$_o$ was involved in Fz signaling at the plasma membrane, but not in endosomes. To investigate this possibility, we coexpressed Rab5 and Gα$_o$ and tested the outcome of Wg-Fz signaling in *Drosophila* wings. In contrast to the positive cooperation of Rab5 and Gα$_o$ in PCP, we found that Gα$_o$ efficiently suppressed the activation of Wg signaling that was induced by Rab5 (Fig. 6, F and G), similar to the effects of the recycling GTPases, Rab4 and Rab11 (Fig. 5, A to D), and reduction in the amounts of Fz proteins (Fig. 6, F and H, also see below). Thus, Gα$_o$ prevented enhanced, Rab5-dependent activation of the Wg pathway, possibly through Rab4-mediated stimulation of recycling of the Wg-Fz ligand-receptor complexes to the plasma membrane.

The effects of Rab5 on Fz signaling and its cooperation with Gα$_o$ depend on the presence of Fz proteins

Because Rab5 controls early endocytic events and because the internalization and relocalization of Fz1 are important steps in the establishment of PCP (30, 31), we reasoned that Gα$_o$-mediated activation of Rab5 might feed back onto Fz1 and trigger its endocytosis. To investigate this possibility, we repeated some of our earlier experiments in the absence of Fz1. Any ge-

netic interaction between Gα$_o$[Q205L] and Rab5 was lost in the *fz1*$^{-/-}$ genetic background. We did not observe any increase in the ability of Gα$_o$[Q205L] to induce multiple wing hairs when Rab5 was coexpressed; removal of one gene copy of *Rab5* did not reduce the potency of Gα$_o$[Q205L] (Fig. 6I). Similarly, the ability of Rab5 to induce multiple wing hairs was reduced in the *fz1*$^{+/-}$ background and lost in the *fz1* homozygous mutant background (Fig. 6J). Proteins involved in the establishment of PCP can be divided into two groups: those involved in the relocalization of Fz1 to the cellular distal tips to delineate the future site of hair initiation (30), and those "execution" proteins that activate actin polymerization to induce hair growth (23, 25). Members of the first group are unable to act without Fz1, whereas members of the second group retain their activity even when Fz1 is absent (11, 58). Thus, the inability of Rab5 to affect the formation of multiple wing hairs in the absence of Fz1 suggested that Rab5 must feed back on Fz1 to regulate the establishment of PCP instead of being a downstream transducer that links Fz1 signaling and the cytoskeleton.

Multiple wing hairs can be induced by an increase in the abundance of Fz1 (40), which possibly leads to a diffuse distribution of Fz1, thus inducing multiple sites of hair growth (30). To test whether a more diffuse localization of Fz1 determined the formation of multiple hairs in our experiments, we expressed Fz1-GFP (30) at low abundance in *Drosophila* wings. We reported previously that overexpression of Gα$_o$ induces a diffuse distribution of Fz1-GFP, which promotes the formation of multiple wing hairs (11). In contrast, we found that Gα$_o$[Q205L] did not induce a diffuse distribution of Fz1-GFP (Fig. 6K), suggesting that the activated form of Gα$_o$ acted on some downstream components of Fz1 signaling to stimulate multiple sites of hair growth, but had no substantial effect on Fz1 itself. Similarly, expression of Rab5 alone was not sufficient to influence the normal zigzag pattern of Fz1-GFP (Fig. 6L). However, coexpression of Gα$_o$[Q205L] and Rab5 affected the localization of Fz1 (Fig. 6M). Thus, the synergy between Gα$_o$[Q205L] and Rab5 in inducing the formation of multiple wing hairs correlated with a diffuse localization of Fz1. In wings from *UASGαo[Q205L];UASRab5* flies, Fz1-GFP was often observed in bright foci (Fig. 6M). We hypothesize that the coexpression of Gα$_o$[Q205L] and Rab5 induces the increased production of Fz1-containing endosomes, which prevents the normal proximo-distal transport of Fz1 and thus strongly induces the formation of multiple wing hairs.

Similar to the situation seen in PCP, the ability of Rab5 to induce the formation of ectopic wing margin bristles was reduced upon the removal, or even a reduction in the amounts, of Fz1 or Fz2 (Fig. 6, F and H). In Wg signaling, enhanced activation of the downstream components of the pathway can produce dominant phenotypes even in the absence of Fz proteins (26). The dependence on the presence of Fz protein of the ability of Rab5[Q88L] to induce dominant activation of the pathway suggests that Rab5 acts epistatically "upstream" of Fz1 and Fz2; that is, that Rab5 feeds back to Fz proteins, most likely to cause their internalization and thus activate the pathway. These observations collectively demonstrate that the activity of Rab5 in Fz-mediated pathways is receptor-dependent, suggesting a positive feedback between the Gα$_o$-dependent activation of Rab5 and Fz proteins. Overall, our experiments reveal a direct and functional interaction between the heterotrimeric G protein G$_o$ and Rab5 that is required for proper signaling by members of the Fz family of GPCRs. We speculate that other G$_o$-coupled GPCRs may similarly rely on an interaction between Gα$_o$ and Rab5 for their signaling.

DISCUSSION

Regulated trafficking of GPCRs is important for their signaling (15, 16). Rab5-dependent endocytosis of GPCRs constitutes the first step in terminating the GPCR signal when endocytosis is followed by transport of the receptor to late endosomes and then to lysosomes for degradation (59). However, the recycling of GPCRs back to the plasma membrane is also

a widespread phenomenon. Fast recycling of receptors is mediated by Rab4, whereas slower recycling is mediated by Rab11 (*14*, *17*). Different GPCRs follow different trafficking and recycling pathways, which can be regulated by modifications of the GPCR (*60*). Further, controlled or directed recycling of GPCRs is often used to enhance signaling in polarized cells, for example, in epithelial or migrating cells (*61*, *62*).

An important question about the Rab-dependent trafficking of GPCRs is how the regulation and specificity of these processes is achieved. The conventional view is that Rabs participate nonspecifically in the receptor trafficking. For example, it is assumed that specificity in endocytosis is first achieved by GPCR kinases and arrestins (*63*), and that Rab5 is recruited at a later stage to promote the formation of clathrin-coated vesicles (*14*). However, because the signaling of different receptors depends differently on various Rab proteins, direct interactions between GPCRs and Rab proteins may be expected; indeed, a few such cases are known. For example, an

interaction between Rab5 and the angiotensin II type 1A receptor leads to the activation of Rab5 in vivo and thus might directly stimulate endocytosis of the receptor (*42*). Another example is the binding of the β_2-adrenergic receptor to Rab11, which is required for proper recycling of the receptor (*64*). Subunits of heterotrimeric G proteins might also be thought of as potential contact partners of Rab proteins that could regulate the specificity of GPCR trafficking. Only one such case has been reported so far: a direct interaction between Rab11 and the $G\beta\gamma$ heterodimer (*65*). However, because $G\beta\gamma$ dimers are promiscuous in their interactions (*66*), this interaction is unlikely to bring specificity to the regulation of GPCR trafficking.

We showed that receptors of the Fz family interacted with Rab5 in vitro and activated Rab5 in *Drosophila* cells. Furthermore, we showed that this activation of Rab5 was mediated by the α subunit of the heterotrimeric G protein, G_o, the immediate transducer of Fz proteins and other GPCRs. $G\alpha_o$ bound directly to Rab5 and Rab4 in vitro and activated Rab5 in vivo by

Fig. 6. Genetic interactions among Rab proteins, $G\alpha_o$, and Fz. (**A** to **D**) Multiple wing hairs induced by $G\alpha_o$ (A) were enhanced by Rab5 (B), Rab11[Q70L] (C), and other Rab proteins (D). Sample size was 8 to 43 wings. (**E** and **I**) $G\alpha_o$[Q205L]-induced multiple wing hairs were enhanced when the abundance of Rab5 was increased, and were reduced when the abundance of Rab5 was decreased, in the presence (E), but not in the absence, of Fz1 (I). For direct comparison of the $fz1^+$ and $fz1^-$ genotypes, the data are presented as percentages, with the number of the multiple wing hairs seen in the $G\alpha o[Q205L]$ wings given as 100%. Sample size was 11 to 28 wings. (**F** to **H**) Rab5[Q88L]-induced ectopic bristles [blue arrowheads in (G) and (H)] were decreased in number upon a reduction in the amounts of Fz1 and Fz2, or upon their complete elimination, and upon coexpression of $G\alpha_o$. Quantification (F) and some examples (G and H) are shown. Sample size was 8 to 21 wings. $G\alpha_o$ induced defects in asymmetric cell division [black arrowhead in (G)] (*94*). (**J**) Rab5-induced multiple wing hairs are suppressed in the $fz1^{H51/+}$ background and lost in the $fz1^{H51}/fz1^{KD4A}$ mutant background; $fz1^{-/-}$ wings alone produce multiple wing hairs. Sample size was 9 to 25 wings. Data are shown as for Fig. 2C. (**K** to **M**) The typical zigzag localization of Fz1-GFP in pupal wings was not affected by $G\alpha_o$[Q205L] (K) or Rab5 (L). When both $G\alpha_o$[Q205L] and Rab5 were coexpressed (M), numerous Fz1-containing intracellular particles were produced (arrowheads). The *MS1096-Gal4* driver was used throughout for overexpression.
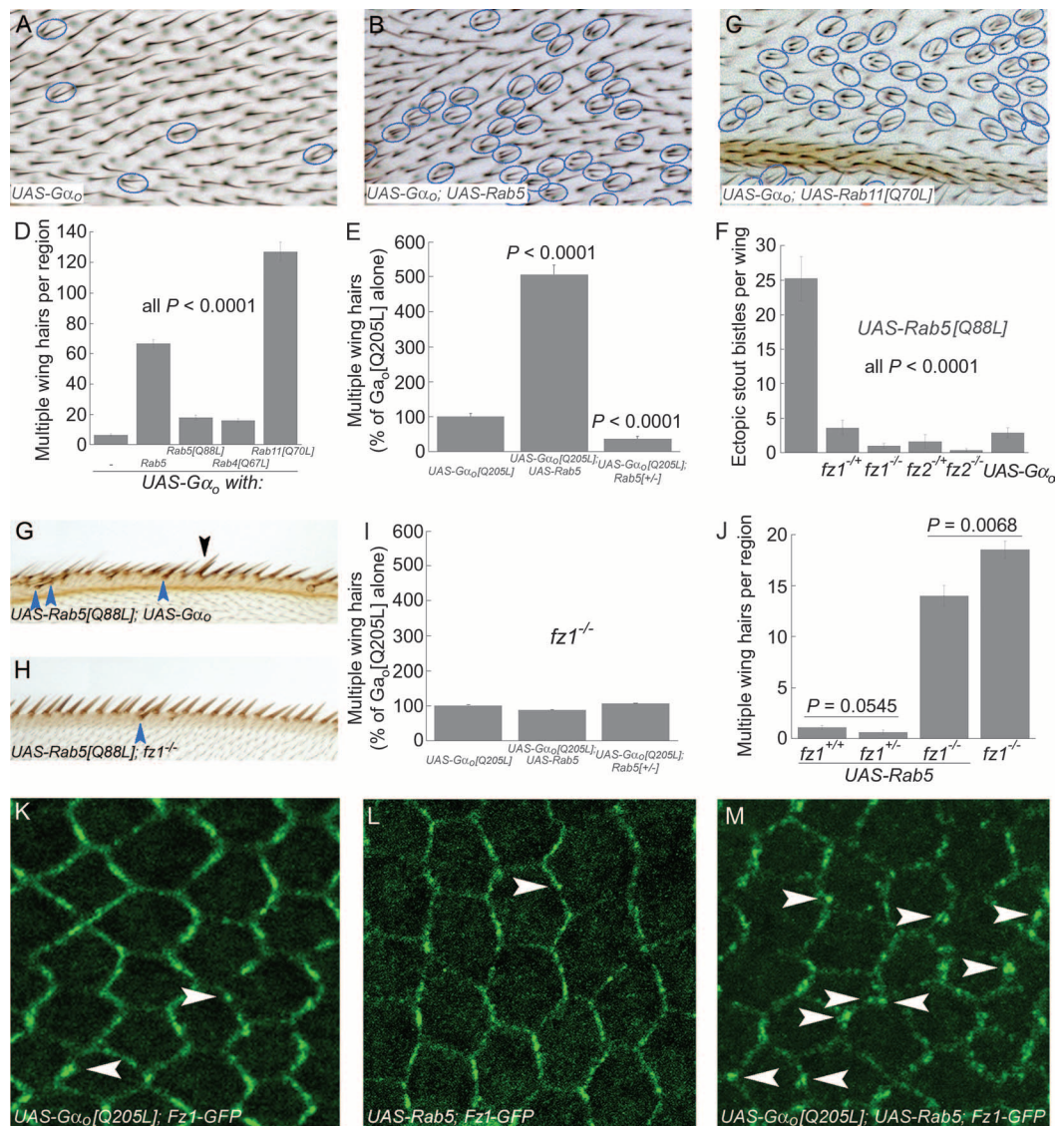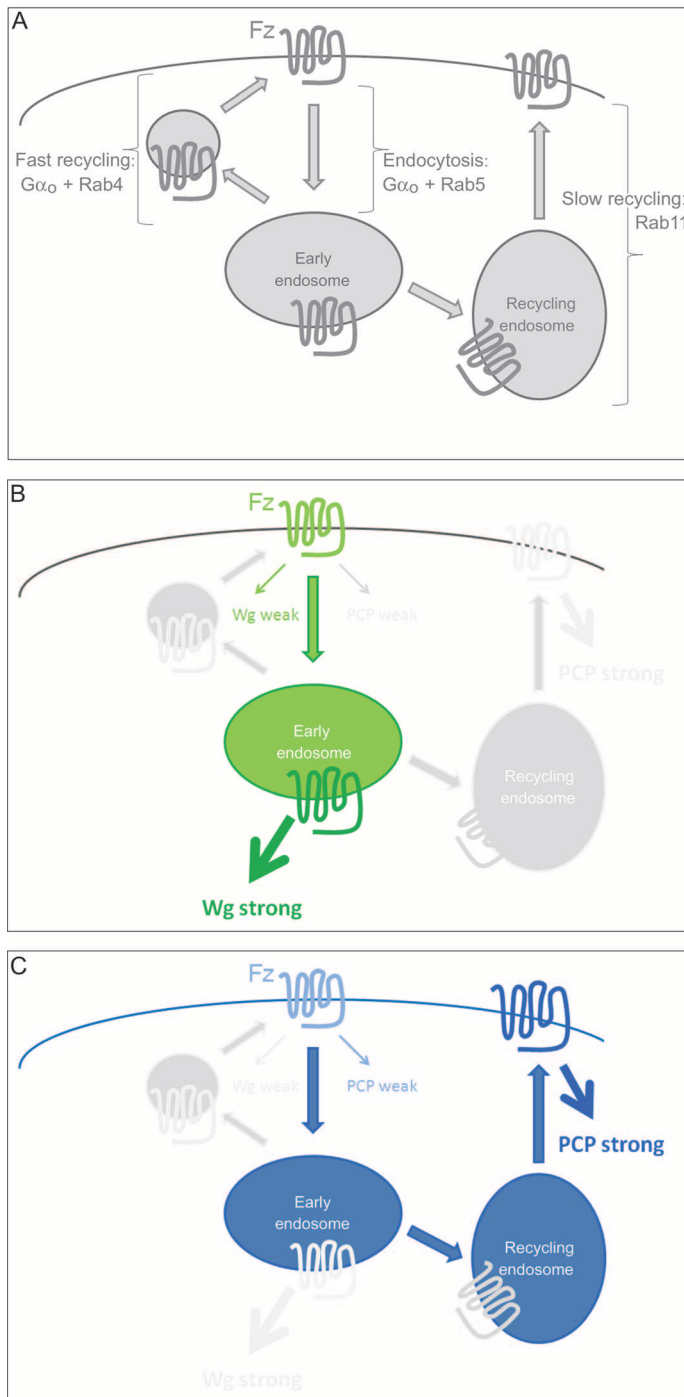
Fig. 7. Model of the interplay among Fz proteins, $G\alpha_o$, and Rab GTPases in Wg and PCP signaling. (**A**) Internalization of Fz from the plasma membrane occurs in a $G\alpha_o$- and Rab5-dependent manner. From early endosomes, Fz has two recycling routes. The first results in fast recycling back to the plasma membrane, which occurs in a $G\alpha_o$- and Rab4-dependent manner. The second route involves slow recycling to the membrane through the recycling endosomes, which is Rab11-dependent. Trafficking to the late endosomes or lysosomes is not considered in this scheme, but may occur. (**B**) In the Wg branch of Fz signaling, signal transduction of plasma membrane–localized Wg-Fz complexes is relatively weak in intensity. Internalization ($G\alpha_o$- and Rab5-dependent) of the ligand-receptor complexes to the early endosomes markedly enhances the strength of signaling. Relocation of the Wg-Fz complexes from the early endosomes through fast ($G\alpha_o$- and Rab4-dependent) or slow (Rab11-dependent) recycling decreases the intensity of Wg signaling. (**C**) In the PCP branch of Fz signaling, relocalization of Fz through early ($G\alpha_o$- and Rab5-dependent) and recycling (Rab11-dependent) endosomes is required for the high-intensity, localized signaling that leads to hair growth.

of many G_o-coupled receptors. Although $G\alpha_o$ activated Rab5 in vivo, we do not know whether it can similarly activate Rab4; however, the strong binding of $G\alpha_o$ to both GTPases in vitro suggests that $G\alpha_o$ might bind to and activate both Rab5 and Rab4 in cells. The predicted outcome of such binding is stimulation of the endocytosis and fast recycling of G_o-coupled GPCRs (Fig. 7A).

Members of the Fz family of GPCRs transduce two different pathways: the Wg pathway, which culminates in gene transcription, and the PCP pathway, which regulates the cytoskeleton (*20*, *25*). Because *Drosophila* Fz1 is fully potent in activating both pathways, the question was raised long ago as to how these two distinct pathways could be activated by the same receptor (*70–72*). Our data provide a model that suggests that the different trafficking routes of Fz proteins may help to mechanically separate the two signaling branches; the molecular basis for this separation is the different roles that $G\alpha_o$ and Rab GTPases play in the two signaling pathways (Fig. 7). $G\alpha_o$ and Rab proteins act as the pointsmen in the split between the Wg and PCP signaling pathways. Whereas the interaction between $G\alpha_o$ and Rab5 was required for both pathways, recycling stimulated the PCP branch but reduced the extent of Wg signaling. More specifically, Rab5-mediated endocytosis of Wg-Fz complexes was required for the high-intensity Wg signaling, but this activity was antagonized by the recycling proteins Rab4 and Rab11. $G\alpha_o$ plays a dual role in this signaling pathway by stimulating Rab5 to endocytose, and Rab4 to recycle, the Wg-Fz complexes (Fig. 7, A and B).

For the PCP signaling branch, our model suggests that $G\alpha_o$, Rab5, and Rab11 cooperate to promote the repeated endocytosis and recycling of Fz1, which is likely accompanied by microtubule-dependent transport of Fz1 vesicles to the distal regions of the wing cell (Fig. 7, A and C). Rab5 was most active in Wg signaling when it was constitutively loaded with GTP. In contrast, wild-type Rab5 was more associated with the PCP phenotypes and had more genetic interactions with $G\alpha_o$ and Rab11 than did constitutively active Rab5. We interpret this difference with the idea that unidirectional endocytosis is required for the maximal strength of the Wg pathway, but that constant recycling is what instead enhances PCP-Fz signaling (Fig. 7, B and C). Overall, our model provides a cell biological and molecular basis to explain the separation of the PCP and Wg signaling cascades.

It should be stressed that the interaction with Rab5 represents only one of several activities of $G\alpha_o$ in Fz signaling. Indeed, the ability of the $G\alpha_o$-Rab5 interaction to affect signaling is dependent on the presence of Fz proteins, whereas activated $G\alpha_o$ induces dominant Wg and PCP phenotypes even in the absence of Fz proteins (*11*). Whereas the Fz-independent targets of

recruiting Rab5 to the plasma membrane. This is the first demonstration of a direct and functional interaction of a G protein α subunit with a Rab GTPase. Our observations have implications for Fz signaling in particular, as well as for GPCR biology in general.

G_o is the predominant G protein in the nervous system of mammals and insects (*2*, *3*). In the growth cone, it constitutes up to 10% of the total amount of plasma membrane protein (*67*). In the brain and other tissues, G_o couples to various GPCRs (*68*, *69*). Thus, the direct and functional interaction between $G\alpha_o$ and Rab GTPases may control the endocytosis and recycling

$G\alpha_o$ in PCP signaling are still unknown, we found a direct effect of $G\alpha_o$ on axin in the Wg pathway (*73*). Thus, $G\alpha_o$ appears to transduce the signal by acting on the downstream components directly in addition to feeding back on Fz proteins through the recruitment and activation of Rab5. This second Rab5-dependent activity of $G\alpha_o$ can be viewed as the amplification step in Fz signaling.

Our data also offer an unexpected clue to the long-observed difference in the activity of Fz1 and Fz2 proteins in Wg signaling. Although both receptors are fully competent to transduce Wg, overexpression of Fz2 results in enhanced activation of the pathway, as seen, for example, by the induction of ectopic wing margin bristles, whereas overexpression of Fz1 does not produce any dominant Wg phenotype (*70*–*72*, *74*, *75*). We propose that this distinction stems from the different basal activities of the two receptors in their capacity to induce endocytosis. Indeed, Fz2 has a strong basal activity in this respect and was only moderately further stimulated by the addition of the Wg ligand (Fig. 2, C and D). In contrast, Fz1 has a moderate basal activity but was stimulated by Wg much more profoundly (fig. S2, C to G). When applied to the situation in the wing, these data suggest that overexpression of Fz2 markedly stimulates endocytosis and thus high-intensity signaling. In contrast, overexpression of Fz1 is insufficient to stimulate endocytosis or enhance activation of the pathway.

In conclusion, our data demonstrate a direct and functional interaction of the small G proteins Rab5 and Rab4 and the heterotrimeric G protein G_o. We further demonstrated the involvement of Rab5 in the PCP-Fz and Wg-Fz signaling pathways in *Drosophila*. We propose that Fz-mediated activation of $G\alpha_o$ leads to the recruitment of Rab5 to the vicinity of the Fz proteins, enhancing receptor endocytosis and thus amplifying the intensity of signaling. The different trafficking routes of Fz-ligand complexes determine the specificity of activation of the Wg and PCP branches of Fz signaling.

MATERIALS AND METHODS

Cloning and protein expression

Drosophila melanogaster CG9139 complementary DNA (cDNA) (clone SD03358) from the Drosophila Genomics Resource Center was amplified by polymerase chain reaction with the primers 5′-GAGATGTCGACGGC-GGCGC-3′ (sense) and 5′-CAGTGACCCAGTCGACAAACGT-3′ (antisense) and cloned into pQE32 by digestion with Sal I. Sequencing revealed a frameshifting mutation in the CG9139 cDNA clone, which was repaired by site-directed mutagenesis with the primers 5′-CGAGAGTCTGGGCGTC-AGCAGCGAGGAG-3′ (sense) and 5′-CTGCTGACGCCCAGACTCTCG-CCATTCAG-3′ (antisense). The resultant plasmid pQE32-CG9139, together with pQE32-Rab5 (*76*) and pQE32-$G\alpha_o$ (*77*), was used for the bacterial expression and purification of N-terminally His$_6$-tagged proteins, as described previously (*76*). The coding sequences of *fz* and *fz2* lacking the predicted signal sequences (Swiss-Prot) were cloned C-terminally to the MBP sequence in the plasmid pMALpoly for plasma membrane–directed bacterial expression, as described previously (*43*). pMAL-5HT2c (*78*) and pMAL-p2 (New England Biolabs) were similarly used for the expression of MBP-5HT2c and MBP. pDEST15Rab plasmids (*79*) were used for the bacterial expression of the GST-tagged *Drosophila* proteins Rab4, Rab5, and Rab11, whereas pGEX-5X3 (GE Healthcare) was used for the expression of GST. Proteins were purified on glutathione resin (GE Healthcare) according to the manufacturer's protocol and stored in phosphate-buffered saline (PBS) containing 1 mM dithiothreitol (DTT), 0.5 mM $MgCl_2$, and 50% glycerol at $-20°C$.

Pull-down experiments

His$_6$-$G\alpha_o$, His$_6$-Rab5, GST, and MBP were individually coupled to CNBr-activated Sepharose 4 Fast Flow (GE Healthcare) according to the manu-

facturer's instructions. Preloading with nucleotide was performed with 1 mM GDP or GTP-γ-S in HKB [10 mM Hepes-NaOH, 135 mM KCl, 10 mM NaCl, 2 mM EGTA (pH 7.5)] supplemented with 5 to 25 mM $MgCl_2$ in case of $G\alpha_o$ and 1 mM EDTA in the case of Rab GTPases. After a 1-hour incubation at room temperature, free nucleotides were removed by serial concentrations in Amicon Ultracel-10 (Millipore) and dilutions with HKB containing 5 mM $MgCl_2$ in the case of soluble proteins, or with multiple dilutions and sedimentations in the case of matrix-immobilized proteins. In experiments with GST-tagged proteins, PBS was used instead of HKB. In pull-down experiments between soluble His$_6$-$G\alpha_o$ and GST-Rabs, nucleotide-preloaded proteins were incubated in equimolar amounts in PBS containing 1 mM DTT and 5 mM $MgCl_2$ (PDM buffer) for 1 hour at room temperature before addition to equal volumes of 50% Ni-NTA agarose (Qiagen) slurry in PDM buffer containing 40 mM imidazole and continued incubation for another 1 hour at room temperature with gentle mixing every 10 min. Free proteins were washed out by serial dilutions or sedimentations in PDM buffer containing 20 mM imidazole until a final 10^7-fold dilution was achieved. The retained proteins were eluted with PBS containing 1 mM DTT and 300 mM imidazole. In pull-down experiments with one of the proteins immobilized on a matrix, incubations were performed for 2 hours at 18°C in HKB containing 0.8 mM CHAPS, 5 mM $MgCl_2$, and 5% glycerol (HCMG buffer). Free proteins were washed out with HCMG as described earlier. For $G\alpha_o$ immobilized on CNBr-Sepharose and Rab5 provided as soluble protein (Fig. 3E), elution of the specifically bound proteins was achieved by nucleotide exchange on Rab5 in the incubation buffer supplemented with 20 mM EDTA and 1 mM guanine nucleotide (GDP was used to elute Rab5–GTP-γ-S, and GTP-γ-S was used to elute Rab5-GDP), as described previously (*80*). $G\alpha_o$ does not exchange its nucleotide under these conditions (*81*). For experiments with *Drosophila* head extracts (*77*) (Fig. 3, G and H) and for experiments in which Rab5 was immobilized on CNBr-Sepharose (Fig. 3F), elution was achieved with 8 M urea. Bacterial membranes expressing Fz1, Fz2, 5HT2c, or MBP were solubilized as described previously (*82*) for 30 min with 10 mM CHAPS at 4°C. After ultracentrifugation at 180,000*g* for 40 min at 4°C, the total protein concentrations in the supernatants were adjusted to 1.8 mg/ml with PBS containing 2 mM EDTA and 10 mM CHAPS. The supernatants were applied to Rab5 or control matrices resuspended in HKB containing 3 mM CHAPS, 0.1% Tween 20, and 5% glycerol (resulting in a final concentration of CHAPS of 3.14 mM) and rotated for 1 hour at 18°C. After any free proteins were washed out with the binding buffer by serial dilutions and sedimentations until a final 10^7-fold dilution was achieved, the retained proteins were eluted with 8 M urea. Proteins were detected by Western blotting analysis with mouse antibody against the histidine tag (Qiagen) at a 1:1000 dilution, mouse antibody against V5 (Invitrogen) at a 1:1000 dilution, rabbit antibody against MBP (New England Biolabs) at a 1:5000 dilution, and horseradish peroxidase–conjugated antibody against GST (GE Healthcare) at a 1:2000 dilution. Gβγ was purified from porcine brains as described (*76*), with the modification that an AlF_4^- preloading step was included, which was performed as described (*83*), before purification on a Phenyl-Sepharose (GE Healthcare) column to ease the removal of Gα subunits. Additionally, Gβγ was eluted in buffer containing 0.5% CHAPS instead of 0.5% Thesit during gel filtration. Fractions were analyzed by Western blotting with rabbit antibody against Gβ1 (Proteintech Europe) at a 1:1000 dilution. The pull-down experiments in the presence of Gβγ were performed as described earlier, except that 8 mM CHAPS was added to prevent nonspecific binding of Gβγ to the matrix.

Drosophila lines

The following *Drosophila* lines were used: *71B-Gal4*, *MS1096-Gal4*, *GMR-Gal4*, *Cg-Gal4*, and *rab5[k08232]* (Bloomington Drosophila Stock Center);

UAS-Rab5, *UAS-Rab5[S43N]*, and *UAS-Rab5-GFP* (*84*); *UAS-Rab5-V5* (a gift from A. Casali); *UAS-Rab5[Q88L]-YFP*, *UAS-Rab5[S43N]-YFP*, *UAS-Rab4[Q67L]-YFP*, and *UAS-Rab11[Q70L]-YFP* (*56*); *UAS-Rab5-RNAi* and *UAS-Gαo-RNAi* [Vienna Drosophila Research Center (*85*)]; *UAS-Gαo* and *UAS-Gαo[Q205L]* (*11*); *UAS-Fz1* (*72*); *fz2[C1]* and *UAS-Fz2* (*86*); *UAS-AxinΔRGS* (*87*); *Vg-Gal4* (*88*); *omb-Gal4* (*89*); *fz1[H51]* and *fz1[KD4A]* (*90*); and *arm-Fz1-GFP* (*30*). All the crosses were performed at 25°C, except for *Vg-Gal4 × UAS-Rab5[S43N]* (Fig. 1, B and G), *Vg-Gal4 × UAS-Rab5-RNAi* (Fig. 1C), and *omb-Gal4 × UAS-Rab5[S43N]-YFP* (Fig. 1H), which were done at 18°C.

Histology

Hemocytes were obtained as previously described (*91*). Briefly, hemolymph from third-instar larvae (5×) was collected into 50 μl of Schneider's *Drosophila* medium (Amimed) supplemented with 10% fetal calf serum (FCS) and was then applied for 30 min at room temperature to 15-mm coverslips precoated with Alcian Blue 8GX (Aldrich), as previously described (*92*). The cells were next fixed with 4% formaldehyde in PBS for 20 min, rinsed three times with 3.5 ml of PBS and permeabilized with 0.5% NP-40 in PBS for 90 s, rinsed twice with PBS, and incubated for 10 min in PBT (PBS + 0.1% Tween 20) before incubation with antibody [1:100 dilution of rabbit antibody against Gαo, Merck catalog no. 371726; 1:50 dilution of rabbit antibody against Rab5 (*84*); and 1:500 dilution of Cy3-coupled antibody against rabbit antibody, Jackson ImmunoResearch] and DAPI (4′,6-diamidino-2-phenylindole, at a 1:10,000 dilution; Sigma) in PBT and analysis by confocal microscopy. Each hemocyte was scanned at several focal planes by confocal microscopy. Giant endosomes were identified in hemocytes as Rab5-containing structures, which appeared in confocal sections as doughnut shapes (Figs. 2 and 3). The number of such structures per hemocyte was counted after analysis at different focal planes. Salivary glands were obtained from third-instar larvae dissected in 0.9% NaCl, fixed in 4% formaldehyde in PBS for 20 min, washed with PBT, and mounted for confocal microscopy. Pupal wings were obtained 30 hours after formation of the puparium and processed as described previously (*11*). To analyze the plasma membrane localization of Rab5[S43N]-YFP in salivary glands, we scanned each gland at several focal planes by confocal microscopy. For each cell, the focal plane corresponding to maximal nuclear staining was next selected. At this focal plane, the presence or absence of Rab5[S43N]-YFP at each of the borders of this cell with its neighbors was assessed according to a three-point scale: complete localization, partial localization, or no localization. Identical microscope settings were used for the different genotypes under comparison. Five glands from different larvae were analyzed for each genotype, with ~30 cells analyzed per gland, with the average number of cell-to-cell contacts being five (ranging from three to six).

Kinetics of in vitro G protein activation

His$_6$-Gαo was preloaded with 1 mM GTP-γ-S as described earlier and exchanged into HKB containing 2 mM MgCl$_2$ with Amicon Ultracel-10, along with His$_6$-CG9139. His$_6$-Rab5 (0.5 μM) in HKB containing 2 mM MgCl$_2$ alone or with a 10-fold molar excess of Gαo–GTP-γ-S was pipetted in the final volume of 50 μl into a black 96-well FLUOTRAC 200 (Greiner Bio-One). The experiment was initiated by the addition of 50 μl of 0.5 μM BODIPY-FL-GTP (Invitrogen) in HKB containing 2 mM MgCl$_2$. The kinetics of fluorescence increase was monitored with the VICTOR3 multiwell reader (Perkin Elmer). CG9139 was used in different concentrations (2 to 100% of the molar amount of Rab5). Activation of Rab5 by solubilized Fz proteins, with or without purified Wg (10 nM), was performed in the presence of 3.14 mM CHAPS. The Gαo activation assay was performed with BODIPY–GTP-γ-S (Invitrogen) as described previously (*77*).

Endocytosis assays

Hemolymph was collected as described earlier, and 50 μl was applied for 30 min at 4°C to each of two 15-mm coverslips precoated with Cultrex Poly-L-Lysine (Trevigen) placed in six-well plates. The 10-min pulse times were started with the addition of 50 μl of precooled (at 4°C) 1 mM Texas Red–conjugated dextran [lysine fixable, M_r (relative molecular mass) 3000; Invitrogen] dissolved in Schneider's medium supplemented with purified Wg to 2 nM (coverslip 1) or Wg control buffer (coverslip 2). The pulse was stopped by washing twice with 3.5 ml of ice-cold PBS, and the chase was started upon the addition of 3.5 ml of PBS (at room temperature) and continued for 20 min at 25°C. The cells were next fixed with 4% formaldehyde in PBS for 20 min, and the coverslips were rinsed three times with 3.5 ml of PBS and mounted for microscopy in Moviol. Wg was purified from conditioned medium as described previously (*93*), which yielded a final stock concentration of 100 nM. S2 cells constitutively expressing *Drosophila* Wg (S2-Tub-Wg, Drosophila Genomics Resource Center) were grown in 150 ml of Schneider's medium supplemented with 10% FCS (HyClone) and 2 mM L-glutamine (Invitrogen) for 3 days. The conditioned medium was harvested by centrifugation at 800*g* for 5 min, and the cell pellet was resuspended in 150 ml of fresh Schneider's medium. After 3 days of additional growth, the second batch of medium was collected and pooled with the first. The medium was filtered through a 1-μm glass fiber filter (Pall). The filtrate was adjusted to 50 mM Hepes (pH 7.5) and 1% Triton X-100, refiltered through 0.22-μm nitrocellulose filters (Millipore), and applied to a 5-ml Blue Sepharose column equilibrated with 50 mM Hepes (pH 7.5), 1% Triton X-100, and 150 mM NaCl. The column was washed with two column volumes of the equilibration buffer and then with two volumes of 50 mM Hepes (pH 7.5), 1% CHAPS, and 150 mM NaCl. Wg was eluted in one step with buffer containing 50 mM Hepes (pH 7.5), 1% CHAPS, and 1500 mM NaCl. Fractions were analyzed by Western blotting with mouse antibody against Wg (Developmental Studies Hybridoma Bank) at a 1:2000 dilution.

SUPPLEMENTARY MATERIALS

REFERENCES AND NOTES

1. A. G. Gilman, G proteins: Transducers of receptor-generated signals. *Annu. Rev. Biochem.* **56**, 615–649 (1987).
2. P. C. Sternweis, J. D. Robishaw, Isolation of two proteins with high affinity for guanine nucleotides from membranes of bovine brain. *J. Biol. Chem.* **259**, 13806–13813 (1984).
3. W. J. Wolfgang, F. Quan, P. Goldsmith, C. Unson, A. Spiegel, M. Forte, Immunolocalization of G protein α-subunits in the *Drosophila* CNS. *J. Neurosci.* **10**, 1014–1024 (1990).
4. M. Jiang, M. S. Gold, G. Boulay, K. Spicher, M. Peyton, P. Brabet, Y. Srinivasan, U. Rudolph, G. Ellison, L. Birnbaumer, Multiple neurological abnormalities in mice deficient in the G protein G$_o$. *Proc. Natl. Acad. Sci. U.S.A.* **95**, 3269–3274 (1998).
5. J. Ferris, H. Ge, L. Liu, G. Roman, G$_o$ signaling is required for *Drosophila* associative learning. *Nat. Neurosci.* **9**, 1036–1040 (2006).
6. D. Valenzuela, X. Han, U. Mende, C. Fankhauser, H. Mashimo, P. Huang, J. Pfeffer, E. J. Neer, M. C. Fishman, Gαo is necessary for muscarinic regulation of Ca^{2+} channels in mouse heart. *Proc. Natl. Acad. Sci. U.S.A.* **94**, 1727–1732 (1997).
7. F. Frémion, M. Astier, S. Zaffran, A. Guillèn, V. Homburger, M. Sémériva, The heterotrimeric protein Go is required for the formation of heart epithelium in *Drosophila*. *J. Cell Biol.* **145**, 1063–1076 (1999).

8. T. Liu, X. Liu, H. Wang, R. T. Moon, C. C. Malbon, Activation of rat Frizzled-1 promotes Wnt signaling and differentiation of mouse F9 teratocarcinoma cells via pathways that require Gα_q and Gα_o function. *J. Biol. Chem.* **274**, 33539–33544 (1999).

9. X. Liu, T. Liu, D. C. Slusarski, J. Yang-Snyder, C. C. Malbon, R. T. Moon, H. Wang, Activation of a Frizzled-2/β-adrenergic receptor chimera promotes Wnt signaling and differentiation of mouse F9 teratocarcinoma cells via Gαo and Gαt. *Proc. Natl. Acad. Sci. U.S.A.* **96**, 14383–14388 (1999).

10. T. Liu, A. J. DeCostanzo, X. Liu, H. Wang, S. Hallagan, R. T. Moon, C. C. Malbon, G protein signaling from activated rat Frizzled-1 to the β-catenin–Lef-Tcf pathway. *Science* **292**, 1718–1722 (2001).

11. V. L. Katanaev, R. Ponzielli, M. Sémériva, A. Tomlinson, Trimeric G protein-dependent Frizzled signaling in *Drosophila*. *Cell* **120**, 111–122 (2005).

12. X. Liu, J. S. Rubin, A. R. Kimmel, Rapid, Wnt-induced changes in GSK3β associations that regulate β-catenin stabilization are mediated by Gα proteins. *Curr. Biol.* **15**, 1989–1997 (2005).

13. D. Egger-Adam, V. L. Katanaev, Trimeric G protein-dependent signaling by Frizzled receptors in animal development. *Front. Biosci.* **13**, 4740–4755 (2008).

14. M. Zerial, H. McBride, Rab proteins as membrane organizers. *Nat. Rev. Mol. Cell Biol.* **2**, 107–117 (2001).

15. J. L. Seachrist, S. S. Ferguson, Regulation of G protein-coupled receptor endocytosis and trafficking by Rab GTPases. *Life Sci.* **74**, 225–235 (2003).

16. J. L. Rosenfeld, B. J. Knoll, R. H. Moore, Regulation of G-protein-coupled receptor activity by rab GTPases. *Receptors Channels* **8**, 87–97 (2002).

17. B. Sönnichsen, S. De Renzis, E. Nielsen, J. Rietdorf, M. Zerial, Distinct membrane domains on endosomes in the recycling pathway visualized by multicolor imaging of Rab4, Rab5, and Rab11. *J. Cell Biol.* **149**, 901–914 (2000).

18. M. Miaczynska, L. Pelkmans, M. Zerial, Not just a sink: Endosomes in control of signal transduction. *Curr. Opin. Cell Biol.* **16**, 400–406 (2004).

19. M. von Zastrow, A. Sorkin, Signaling on the endocytic pathway. *Curr. Opin. Cell Biol.* **19**, 436–445 (2007).

20. B. T. MacDonald, K. Tamai, X. He, Wnt/β-catenin signaling: Components, mechanisms, and diseases. *Dev. Cell* **17**, 9–26 (2009).

21. C. V. Cabrera, M. C. Alonso, P. Johnston, R. G. Phillips, P. A. Lawrence, Phenocopies induced with antisense RNA identify the *wingless* gene. *Cell* **50**, 659–663 (1987).

22. F. Rijsewijk, M. Schuermann, E. Wagenaar, P. Parren, D. Weigel, R. Nusse, The *Drosophila* homolog of the mouse mammary oncogene *int*-1 is identical to the segment polarity gene *wingless*. *Cell* **50**, 649–657 (1987).

23. M. Fanto, H. McNeill, Planar polarity from flies to vertebrates. *J. Cell Sci.* **117**, 527–533 (2004).

24. I. Roszko, A. Sawada, L. Solnica-Krezel, Regulation of convergence and extension movements during vertebrate gastrulation by the Wnt/PCP pathway. *Semin. Cell Dev. Biol.* **20**, 986–997 (2009).

25. P. N. Adler, Planar signaling and morphogenesis in *Drosophila*. *Dev. Cell* **2**, 525–535 (2002).

26. C. M. Chen, G. Struhl, Wingless transduction by the Frizzled and Frizzled2 proteins of *Drosophila*. *Development* **126**, 5441–5452 (1999).

27. C. R. Vinson, S. Conover, P. N. Adler, A *Drosophila* tissue polarity locus encodes a protein containing seven potential transmembrane domains. *Nature* **338**, 263–264 (1989).

28. V. L. Katanaev, A. Tomlinson, Multiple roles of a trimeric G protein in *Drosophila* cell polarization. *Cell Cycle* **5**, 2464–2472 (2006).

29. G. H. Kim, J. K. Han, Essential role for β-arrestin 2 in the regulation of *Xenopus* convergent extension movements. *EMBO J.* **26**, 2513–2526 (2007).

30. D. I. Strutt, Asymmetric localization of Frizzled and the establishment of cell polarity in the *Drosophila* wing. *Mol. Cell* **7**, 367–375 (2001).

31. Y. Shimada, S. Yonemura, H. Ohkura, D. Strutt, T. Uemura, Polarized transport of Frizzled along the planar microtubule arrays in *Drosophila* wing epithelium. *Dev. Cell* **10**, 209–222 (2006).

32. E. Nielsen, F. Severin, J. M. Backer, A. A. Hyman, M. Zerial, Rab5 regulates motility of early endosomes on microtubules. *Nat.* **1**, 376–382 (1999).

33. J. T. Blitzer, R. Nusse, A critical role for endocytosis in Wnt signaling. *BMC Cell Biol.* **7**, 28 (2006).

34. E. S. Seto, H. J. Bellen, Internalization is required for proper Wingless signaling in *Drosophila melanogaster*. *J. Cell Biol.* **173**, 95–106 (2006).

35. V. L. Katanaev, G. P. Solis, G. Hausmann, S. Buestorf, N. Katanayeva, Y. Schrock, C. A. Stuermer, K. Basler, Reggie-1/flotillin-2 promotes secretion of the long-range signalling forms of Wingless and Hedgehog in *Drosophila*. *EMBO J.* **27**, 509–521 (2008).

36. J. P. Couso, S. A. Bishop, A. Martinez Arias, The wingless signalling pathway and the patterning of the wing margin in *Drosophila*. *Development* **120**, 621–636 (1994).

37. H. Jafar-Nejad, A. C. Tien, M. Acar, H. J. Bellen, Senseless and Daughterless confer neuronal identity to epithelial cells in the *Drosophila* wing margin. *Development* **133**, 1683–1692 (2006).

38. R. Nolo, L. A. Abbott, H. J. Bellen, Senseless, a Zn finger transcription factor, is necessary and sufficient for sensory organ development in *Drosophila*. *Cell* **102**, 349–362 (2000).

39. H. Lu, D. Bilder, Endocytic control of epithelial polarity and proliferation in *Drosophila*. *Nat. Cell Biol.* **7**, 1232–1239 (2005).

40. R. E. Krasnow, P. N. Adler, A single *frizzled* protein has a dual function in tissue polarity. *Development* **120**, 1883–1893 (1994).

41. H. Stenmark, G. Vitale, O. Ullrich, M. Zerial, Rabaptin-5 is a direct effector of the small GTPase Rab5 in endocytic membrane fusion. *Cell* **83**, 423–432 (1995).

42. J. L. Seachrist, S. A. Laporte, L. B. Dale, A. V. Babwah, M. G. Caron, P. H. Anborgh, S. S. Ferguson, Rab5 association with the angiotensin II type 1A receptor promotes Rab5 GTP binding and vesicular fusion. *J. Biol. Chem.* **277**, 679–685 (2002).

43. V. L. Katanaev, S. Buestorf, Frizzled proteins are *bona fide* G protein-coupled receptors. *Nat. Precedings* (2009); http://hdl.handle.net/10101/npre.2009.2765.1.

44. W. R. Leifert, A. L. Aloia, O. Bucco, R. V. Glatz, E. J. McMurchie, G-protein-coupled receptors in drug discovery: Nanosizing using cell-free technologies and molecular biology approaches. *J. Biomol. Screen.* **10**, 765–779 (2005).

45. D. P. McEwen, K. R. Gee, H. C. Kang, R. R. Neubig, Fluorescent BODIPY-GTP analogs: Real-time measurement of nucleotide binding to G proteins. *Anal. Biochem.* **291**, 109–117 (2001).

46. H. Horiuchi, R. Lippe, H. M. McBride, M. Rubino, P. Woodman, H. Stenmark, V. Rybin, M. Wilm, K. Ashman, M. Mann, M. Zerial, A novel Rab5 GDP/GTP exchange factor complexed to Rabaptin-5 links nucleotide exchange to effector recruitment and function. *Cell* **90**, 1149–1159 (1997).

47. E. García-García, P. L. García-García, C. Rosales, An fMLP receptor is involved in activation of phagocytosis by hemocytes from specific insect species. *Dev. Comp. Immunol.* **33**, 728–739 (2009).

48. A. Kikuchi, H. Yamamoto, A. Sato, Selective activation mechanisms of Wnt signaling pathways. *Trends Cell Biol.* **19**, 119–129 (2009).

49. L. Giot, J. S. Bader, C. Brouwer, A. Chaudhuri, B. Kuang, Y. Li, Y. L. Hao, C. E. Ooi, B. Godwin, E. Vitols, G. Vijayadamodar, P. Pochart, H. Machineni, M. Welsh, Y. Kong, B. Zerhusen, R. Malcolm, Z. Varrone, A. Collis, M. Minto, S. Burgess, L. McDaniel, E. Stimpson, F. Spriggs, J. Williams, K. Neurath, N. Ioime, M. Agee, E. Voss, K. Furtak, R. Renzulli, N. Aanensen, S. Carrolla, E. Bickelhaupt, Y. Lazovatsky, A. DaSilva, J. Zhong, C. A. Stanyon, R. L. Finley Jr., K. P. White, M. Braverman, T. Jarvie, S. Gold, M. Leach, J. Knight, R. A. Shimkets, M. P. McKenna, J. Chant, J. M. Rothberg, A protein interaction map of *Drosophila melanogaster*. *Science* **302**, 1727–1736 (2003).

50. M. J. Cismowski, C. Ma, C. Ribas, X. Xie, M. Spruyt, J. S. Lizano, S. M. Lanier, E. Duzic, Activation of heterotrimeric G-protein signaling by a Ras-related protein. Implications for signal integration. *J. Biol. Chem.* **275**, 23421–23424 (2000).

51. M. J. Cismowski, A. Takesono, C. Ma, J. S. Lizano, X. Xie, H. Fuernkranz, S. M. Lanier, E. Duzic, Genetic screens in yeast to identify mammalian nonreceptor modulators of G-protein signaling. *Nat. Biotechnol.* **17**, 878–883 (1999).

52. J. E. Slessareva, S. M. Routt, B. Temple, V. A. Bankaitis, H. G. Dohlman, Activation of the phosphatidylinositol 3-kinase Vps34 by a G protein α subunit at the endosome. *Cell* **126**, 191–203 (2006).

53. N. Katanayeva, D. Kopein, R. Portmann, D. Hess, V. L. Katanaev, Competing activities of trimeric G proteins in *Drosophila* wing maturation. *PLoS One* 10.1371/journal.pone.0012331 (2010).

54. D. Egger-Adam, V. L. Katanaev, The trimeric G protein Go inflicts a double impact on axin in the Wnt/Frizzled signaling pathway. *Dev. Dyn.* **239**, 168–183 (2009).

55. M. C. Seabra, C. Wasmeier, Controlling the location and activation of Rab GTPases. *Curr. Opin. Cell Biol.* **16**, 451–457 (2004).

56. J. Zhang, K. L. Schulze, P. R. Hiesinger, K. Suyama, S. Wang, M. Fish, M. Acar, R. A. Hoskins, H. J. Bellen, M. P. Scott, Thirty-one flavors of *Drosophila* Rab proteins. *Genetics* **176**, 1307–1322 (2007).

57. C. G. Winter, B. Wang, A. Ballew, A. Royou, R. Karess, J. D. Axelrod, L. Luo, *Drosophila* Rho-associated kinase (Drok) links Frizzled-mediated planar cell polarity signaling to the actin cytoskeleton. *Cell* **105**, 81–91 (2001).

58. L. L. Wong, P. N. Adler, Tissue polarity genes of *Drosophila* regulate the subcellular location for prehair initiation in pupal wing cells. *J. Cell Biol.* **123**, 209–221 (1993).

59. S. S. Ferguson, Evolving concepts in G protein-coupled receptor endocytosis: The role in receptor desensitization and signaling. *Pharmacol. Rev.* **53**, 1–24 (2001).

60. F. Wang, X. Chen, X. Zhang, L. Ma, Phosphorylation state of μ-opioid receptor determines the alternative recycling of receptor via Rab4 or Rab11 pathway. *Mol. Endocrinol.* **22**, 1881–1892 (2008).

61. M. C. Jones, P. T. Caswell, J. C. Norman, Endocytic recycling pathways: Emerging regulators of cell migration. *Curr. Opin. Cell Biol.* **18**, 549–557 (2006).

62. D. Hoekstra, D. Tyteca, S. C. van IJzendoorn, The subapical compartment: A traffic center in membrane polarity development. *J. Cell Sci.* **117**, 2183–2192 (2004).

63. M. T. Drake, S. K. Shenoy, R. J. Lefkowitz, Trafficking of G protein–coupled receptors. *Circ. Res.* **99**, 570–582 (2006).

64. A. Parent, E. Hamelin, P. Germain, J. L. Parent, Rab11 regulates the recycling of the β2-adrenergic receptor through a direct interaction. *Biochem. J.* **418**, 163–172 (2009).

65. A. García-Regalado, M. L. Guzmán-Hernández, I. Ramírez-Rangel, E. Robles-Molina, T. Balla, J. Vázquez-Prado, G. Reyes-Cruz, G protein-coupled receptor-promoted trafficking of Gβ1γ2 leads to AKT activation at endosomes via a mechanism mediated by Gβ1γ2-Rab11a interaction. *Mol. Biol. Cell* **19**, 4188–4200 (2008).

66. D. E. Clapham, E. J. Neer, G protein βγ subunits. *Annu. Rev. Pharmacol. Toxicol.* **37**, 167–203 (1997).

67. S. M. Strittmatter, D. Valenzuela, T. E. Kennedy, E. J. Neer, M. C. Fishman, G₀ is a major growth cone protein subject to regulation by GAP-43. *Nature* **344**, 836–841 (1990).

68. S. Offermanns, G-proteins as transducers in transmembrane signalling. *Prog. Biophys. Mol. Biol.* **83**, 101–130 (2003).

69. K. D. Bromberg, R. Iyengar, J. C. He, Regulation of neurite outgrowth by $G_{i/o}$ signaling pathways. *Front. Biosci.* **13**, 4544–4557 (2008).

70. M. Boutros, J. Mihaly, T. Bouwmeester, M. Mlodzik, Signaling specificity by Frizzled receptors in *Drosophila*. *Science* **288**, 1825–1828 (2000).

71. E. J. Rulifson, C. H. Wu, R. Nusse, Pathway specificity by the bifunctional receptor Frizzled is determined by affinity for Wingless. *Mol. Cell* **6**, 117–126 (2000).

72. W. R. Strapps, A. Tomlinson, Transducing properties of *Drosophila* Frizzled proteins. *Development* **128**, 4829–4835 (2001).

73. D. Egger-Adam, V. L. Katanaev, The trimeric G protein Go inflicts a double impact on axin in the Wnt/Frizzled signaling pathway. *Dev. Dyn.* **239**, 168–183 (2010).

74. K. M. Cadigan, M. P. Fish, E. J. Rulifson, R. Nusse, Wingless repression of *Drosophila frizzled 2* expression shapes the Wingless morphogen gradient in the wing. *Cell* **93**, 767–777 (1998).

75. J. Zhang, R. W. Carthew, Interactions between Wingless and DFz2 during *Drosophila* wing development. *Development* **125**, 3075–3085 (1998).

76. A. Koval, D. Kopein, V. Purvanov, V. L. Katanaev, Europium-labeled GTP as a general nonradioactive substitute for [^{35}S]GTPγS in high-throughput G protein studies. *Anal. Biochem.* **397**, 202–207 (2010).

77. D. Kopein, V. L. Katanaev, *Drosophila* GoLoco-protein pins is a target of $G\alpha_o$-mediated G protein–coupled receptor signaling. *Mol. Biol. Cell* **20**, 3865–3877 (2009).

78. F. Mancia, S. Brenner-Morton, R. Siegel, Z. Assur, Y. Sun, I. Schieren, M. Mendelsohn, R. Axel, W. A. Hendrickson, Production and characterization of monoclonal antibodies sensitive to conformation in the 5HT2c serotonin receptor. *Proc. Natl. Acad. Sci. U.S.A.* **104**, 4303–4308 (2007).

79. H. A. Morrison, H. Dionne, T. E. Rusten, A. Brech, W. W. Fisher, B. D. Pfeiffer, S. E. Celniker, H. Stenmark, D. Bilder, Regulation of early endosomal entry by the *Drosophila* tumor suppressors Rabenosyn and Vps45. *Mol. Biol. Cell* **19**, 4167–4176 (2008).

80. S. Christoforidis, H. M. McBride, R. D. Burgoyne, M. Zerial, The Rab5 effector EEA1 is a core component of endosome docking. *Nature* **397**, 621–625 (1999).

81. D. J. Carty, R. Iyengar, Guanosine 5′-(γ-thio)triphosphate binding assay for solubilized G proteins. *Methods Enzymol.* **237**, 38–44 (1994).

82. H. B. Weems, E. Chalecka-Franaszek, T. E. Cote, Solubilization of high-affinity, guanine nucleotide-sensitive μ-opioid receptors from rat brain membranes. *J. Neurochem.* **66**, 1042–1050 (1996).

83. J. J. Tesmer, D. M. Berman, A. G. Gilman, S. R. Sprang, Structure of RGS4 bound to AlF4⁻-activated $G_{i\alpha1}$: Stabilization of the transition state for GTP hydrolysis. *Cell* **89**, 251–261 (1997).

84. T. Wucherpfennig, M. Wilsch-Bräuninger, M. González-Gaitán, Role of *Drosophila* Rab5 during endosomal trafficking at the synapse and evoked neurotransmitter release. *J. Cell Biol.* **161**, 609–624 (2003).

85. G. Dietzl, D. Chen, F. Schnorrer, K. C. Su, Y. Barinova, M. Fellner, B. Gasser, K. Kinsey, S. Oppel, S. Scheiblauer, A. Couto, V. Marra, K. Keleman, B. J. Dickson, A genome-wide transgenic RNAi library for conditional gene inactivation in *Drosophila*. *Nature* **448**, 151–156 (2007).

86. C. M. Chen, W. Strapps, A. Tomlinson, G. Struhl, Evidence that the cysteine-rich domain of *Drosophila* Frizzled family receptors is dispensable for transducing Wingless. *Proc. Natl. Acad. Sci. U.S.A.* **101**, 15961–15966 (2004).

87. K. Willert, C. Y. Logan, A. Arora, M. Fish, R. Nusse, A *Drosophila* Axin homolog, Daxin, inhibits Wnt signaling. *Development* **126**, 4165–4173 (1999).

88. A. J. Simmonds, W. J. Brook, S. M. Cohen, J. B. Bell, Distinguishable functions for *engrailed* and *invected* in anterior-posterior patterning in the *Drosophila* wing. *Nature* **376**, 424–427 (1995).

89. T. Lecuit, W. J. Brook, M. Ng, M. Calleja, H. Sun, S. M. Cohen, Two distinct mechanisms for long-range patterning by Decapentaplegic in the *Drosophila* wing. *Nature* **381**, 387–393 (1996).

90. K. H. Jones, J. Liu, P. N. Adler, Molecular analysis of EMS-induced *frizzled* mutations in *Drosophila melanogaster*. *Genetics* **142**, 205–215 (1996).

91. R. Lanot, D. Zachary, F. Holder, M. Meister, Postembryonic hematopoiesis in *Drosophila*. *Dev. Biol.* **230**, 243–257 (2001).

92. M. Suomalainen, M. Y. Nakano, S. Keller, K. Boucke, R. P. Stidwill, U. F. Greber, Microtubule-dependent plus- and minus end–directed motilities are competing processes for nuclear targeting of adenovirus. *J. Cell Biol.* **144**, 657–672 (1999).

93. K. Willert, J. D. Brown, E. Danenberg, A. W. Duncan, I. L. Weissman, T. Reya, J. R. Yates III, R. Nusse, Wnt proteins are lipid-modified and can act as stem cell growth factors. *Nature* **423**, 448–452 (2003).

94. V. L. Katanaev, A. Tomlinson, Dual roles for the trimeric G protein Go in asymmetric cell division in *Drosophila*. *Proc. Natl. Acad. Sci. U.S.A.* **103**, 6524–6529 (2006).